Spencer Laboratory

Engineering Report

Report No. PT-913

Research and Development of a V-Band
3.2 Millimeter Magnetron

Report Nr. 2

Contract Nr. DA28-043-AMC-00229 (E)

Technical Guidelines MW-15
dated 12 February 1964

Department of the Army Project
Nr. 1P6-22001-A005-04

Final Report
15 August 1964 - 15 February 1965

RAYTHEON COMPANY

MICROWAVE AND POWER TUBE DIVISION

DDC AVAILABILITY NOTICE

RAYTHEON COMPANY
Microwave and Power Tube Division
Microwave Tube Operation
altham, Massachusetts

RESEARCH AND DEVELOPMENT OF A

V-BAND 3.2 MILLIMETER MAGNETRON

Report Nr. 2

Contract Nr. DA28-043-AMC-00229 (E)
Technical Guidelines MW-15 dated 12 February 1964
Department of the Army Project Nr. 1P6-22001-A005-04
Final Report, 15 August 1964 - 15 February 1965

This report was written by R. Plumridge and was edited by
R. Adams

This report has been approved by

J. H. Schussele, Manager
Crossed-Field Oscillator Group

L. L. Clampitt,
Manager of Engineering,
Microwave Tube Operation

TABLE OF CONTENTS

LIST OF ILLUSTRATIONS

LIST OF ILLUSTRATIONS (Continued)

LIST OF TABLES

1.   PURPOSE OF THE PROGRAM

The purpose of the program was to develop a V-band, 3.2 mm, inverted cavity-stabilized magnetron. This 6 month effort was a feasibility study conducted to investigate the problems associated with the design of a 3.2 mm Magnetron. This effort included cold testing of X-band scale models of the anode and with the design and evaluation of a heater-cathode structure and the mode damping assembly. In addition, a V-band model of the tube was cold tested by the conclusion of the study. The program was started on August 15, 1964, and was completed on February 15, 1965.

Specific items of work included in the six month feasibility study are listed below:

1.   Design and layout of the proposed tube.

2.   Development of the X-band anode cavity and damper components in cold test.

3.   Development of a slot mode attenuator for V-band.

4.   Development and test of cathode and heater structures for V-band.

5.   Procurement of 3.2 mm anode.

6.   Development of a V-band output circuit.

7.   Performance of cold test of V-band anode, cavity and output assembly.

2.   ABSTRACT

This final report describes the work performed under Electronics
Command Contract Number DA-28-043-AMC-00229 (E) to develop an inverted
coaxial V-band cavity-stabilized magnetron. The study included the develop-
ment and cold testing of X- and V-band models of the anode, and the design
and testing of critical components of the tube such as the heater cathode assembly
and the mode damper.

A 9-scaled X-band cold test model of the anode, cavity and output
was made and extensively investigated. The fast cyclotron mode intereference
problem was explored. A satisfactory V-band anode was made with E. D. M.
techniques. A good unloaded Q was measured with the V-band anode and a
satisfactory match was obtained with a $\lambda/2$ ceramic window. A practical
magnetic circuit was worked out to provide high magnetic field. An investi-
gation of carburized ceramic dampers was made and, although a satisfactory
damper was not developed during this period, the design of a good damper does
not appear to be a difficult problem. A model of the heater cathode assembly
was constructed for bell jar test and was life tested for a period of 1040 hours.

3. PUBLICATIONS, LECTURES, REPORTS AND CONFERENCES

No publications or lectures pertaining to this program occurred during the report period. The following meetings were held.

Progress Report at USAEL

Date	U. S. Army Participant	Raytheon Participant
9 November 1964	N. Wilson	J. Schussele

Progress Reports at Raytheon

Date	U. S. Army Participants	Raytheon Participants
20 August 1964	E. Kaiser	W. Bower, R. Plumridge
19 September 1964	F. Kaiser	E. Downing, R. Plumridge
29 January 1965	E. Kaiser	E. Downing, R. Plumridge

The purpose of the January 29, 1965, meeting was an over-all review of the technical progress of the program. The future aspects of this phase of the program were also discussed.

4.   FACTUAL DATA

4.1   Introduction

Under the terms of Contract No. DA28-043-AMC-00229 (E), dated 11 August 1964, Raytheon Company has carried out research and development of a V-band 3.2 millimeter wave oscillator as outlined in Electronics Command Technical Guidelines MW-15, dated 12 February 1964, and Raytheon Technical proposal, PRP-1601, dated 7 April 1964.

This program was initiated on 15 August 1964 to develop a V-band inverted cavity-stabilized magnetron. The study program, comprising the six month effort authorized by the above contract, was concerned with the electro-mechanical aspects of the design. Cold test work was conducted on anode, cavity, and output models scaled to X-band for convenience. Critical tube components were also designed and analyzed. A V-band anode was constructed and cold tested toward the end of the period.

4.2   Tube Requirements

The requirements for the tube are given in Table I

TABLE I

TUBE REQUIREMENTS

a.   Electrical Requirements

Frequency	93.75 ±2.0 Gc
Peak power	3 Kw
Duty cycle	0.0003
Efficiency	5%
Pulse width	0.25 μsec

Anode voltage	35 kv (max)
Rf bandwidth	2. 5/tp
Lifetime	50 hr
Output waveguide	circular waveguide desired

b. Mechanical Requirements

Weight	30 lb
Magnet	solenoid or permanent magnet
Cooling	forced air or liquid

4.3   Design Approach

The design selected to meet these requirements is an inverted
coaxial magnetron. A layout drawing of the tube is given in Figure 1.
With this type of tube design, the cathode encompasses the anode, and the
anode cavities are coupled to a central stabilizing cavity through slots at
the back of alternate cavities. The internal cavity is the principle .re-
quency determining element of the tube. It is also responsible for the high
degree of stabilization for the tube. As indicated on the layout drawing,
the cavity is a circular cylinder tuned by means of a plate which forms one
end of the cavity. The cavity operates in the TE_{011} mode. The cavity
plate serves as an iris, coupling the energy of the cavity to a circular
TE_{01} output line. A half wavelength ceramic window is part of
the vacuum envelope. The cathode is an impregnated tungsten matrix type , and the
cathode heater assembly is supported by means of a ceramic isolator
which connects it to the tuner pole of the tube. The cathode is adjustable
by means of four set screws which press against the assembly through a
diaphragm set in the wall of the tube. Alignment of the cathode and anode,
which is critical, can be accomplished with this adjustment device.
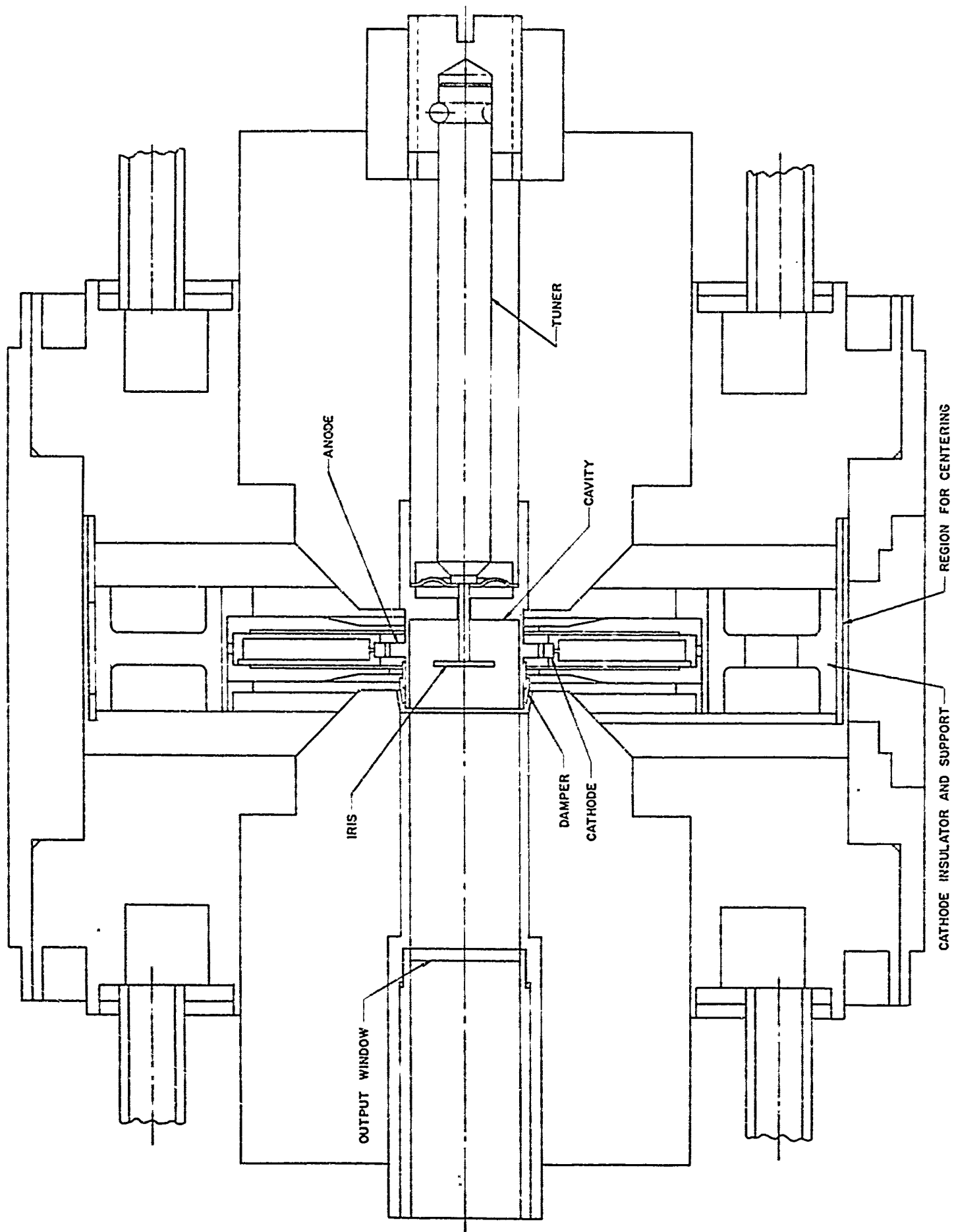
Figure 1   Tube Layout (V-Band)

TUNER

ANODE

CAVITY

REGION FOR CENTERING

IRIS

DAMPER

CATHODE

CATHODE INSULATOR AND SUPPORT

OUTPUT WINDOW

- 6 -

The principle design parameters of the magnetron are given below in Table II

TABLE II
PRINCIPAL DESIGN PARAMETERS

Cavity ID	0.2105 inch
Wall thickness	0.0080 inch
Radial vane length	0.030 inch
Vane height	0.026 inch
Number of vanes	100
Vane-to-vane spacing	0.009 inch
Vane-to-cathode spacing	0.009 inch
Frequency	93.75 G_c
Characteristic voltage, V_o	5.3 kV
B_o	10.83 Kg
B/B_o	2.12
B	23 Kg
V	17 KV
Peak current	4.0 amperes
Output power	3.0 KW
Operating efficiency	5%

It is believed that the basic tube design set for the above represents a straightforward approach to the development of the 3.2 mm magnetron.

Within the framework of this basic design, it was necessary to determine several critical parameters and to develop reliable component designs. These included damper construction and position, slot length, adjustment of output cou ing to load and reliable heater/cathode design. These items are discussed in the appropriate sections of this report.

4.4   X-Band Cold Test Program

4.4.1   Introduction

It was decided to perform the cold test work at X-band. The
reliability of the cold test results at this band is superior to that at
V-band where the components are extremely small. Thus, modification
of the design could be made and assessed at X-band with good accuracy.
An X-band cold test model was designed and constructed. It was a fre-
quency scaled version (factor 9.2) of the V-band tube.

The X-band cold test model had the design parameters shown in
Table III.

TABLE III
DESIGN PARAMETERS OF X-BAND COLD-TEST MODEL

Anode diameter	2.553 inches
Cathode diameter	2.714 inches
Vane length	0.2585 inch
Vane height	0.2305 inch
Vane thickness	0.040 inch
Gap/vane ratio	1/1
Number of vanes	100

The following is a list of tube characteristics which were exami-
ned at X-band and presumed to scale to V-band.

1.   Mode spectrum of the slotted and unslotted anode.
2.   Slot modes.
3.   Attenuation of unwanted lower order anode modes, slot
     resonances, undesired cavity modes, and other extraneous
     modes.

4. Unloaded Q.

5. Anode-output coupling.

6. Cavity modes.

4.4.2 Analysis of the Multivane Anode Structure

Part of the X-band cold test program was directed towards
obtaining a better understanding of the mode spectrum of the multi-vaned
anode structure which is employed in inverted coaxial magnetrons. This
part of the investigation could be considered an extension of a previous
Raytheon cold test study which was conducted at S-band. The X-band cold
test results corroborated the data at S-band. The X-band data can be
assumed to scale to the design of the V-band coaxial magnetion with a
reasonably good degree of accuracy.

Initially, the unslotted anode-cavity design was examined. This
information served as a basis for the understanding of the slotted anode
structures. The fundamental wave propagated on the unslotted cavity-
anode structure is a forward wave. Figure 2 illustrates the measured
forward mode distribution for the fundamental circuit wave. The highest
resonant frequency of the structure was the π-mode (n = 50) which occurred
at 10.68 Gc. This frequency was very close to the computed π-mode fre-
quency. For computations of the resonant π-mode frequency, the vane cavity
structure was considered a transmission line terminated by a short circuit
at one end and by fringing capacitance on the other end. Resonant fre-
quencies of modes n = 4 through n = 35 were established. These modes
were identified by determining the circumferential distance at the vane
tips between voltage nulls. This method is adequate for locating the
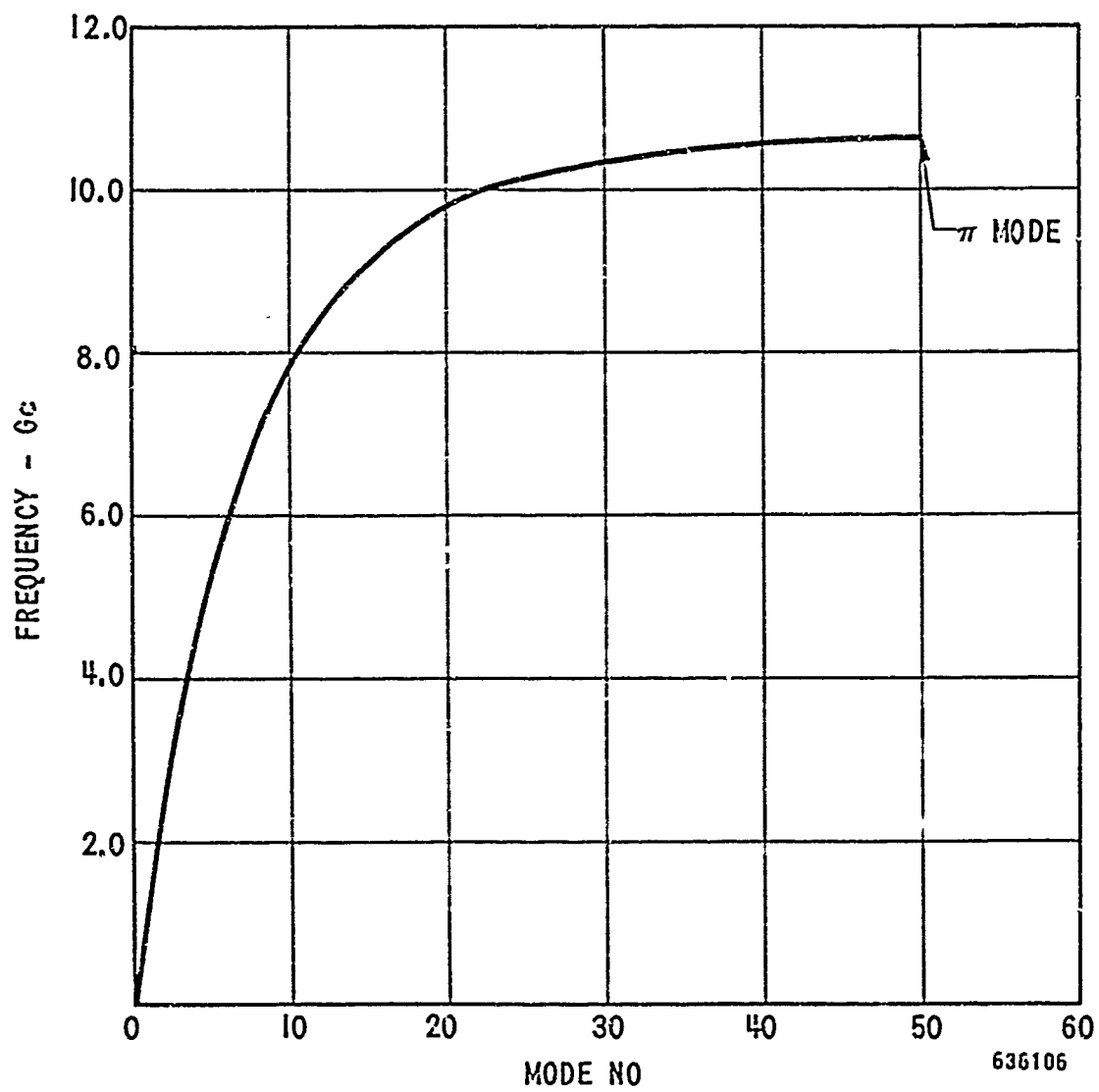resonant frequencies of the lower order modes.

FIGURE 2   X-Band – Unslotted Anode
Mode Spectrum–Fundamental
Forward Circuit Wave

The ω-β curve is plotted in Figure 3 for the unslotted anode, while, in Figure 4, the approximate relative amplitudes of the circuit modes are given for this structure. The amplitude of the circuit modes was detected by two E-probes located 180° apart on the cathode surface and penetrating 0.010 inch into the interaction space. One probe served as the input while the other probe was the detector. Referring to Figure 4, it is observed that the electric fields of the lower order modes are more intense at the cathode surface than are the electric fields of the higher order modes. This result is consistent with the analysis of a multi-vaned anode-cathode structure. At low frequencies (lower order modes), the electric fields exist almost entirely in the interaction space. There are no electric fields in the transverse direction at the vane resonators, and the magnetic fields are constant in the vane region. At low frequencies, the anode-cathode circuit modes are essentially TEM waves that propagate at the velocity of light. At higher frequencies, the propagating modes are more closely associated with the anode structure. Here, transverse electric fields exist at the vane tips. These modes are the slow propagating circuit waves. Their electric field strength at the cathode surface is much weaker than that of the lower order frequency modes.

To gain understanding of the effects of the cavity-anode slots on the mode pattern, the anode was slotted in a succession of three steps. The dimensions of the three slots added to the anode are given in Table IV.

TABLE IV

SLOT DIMENSIONS

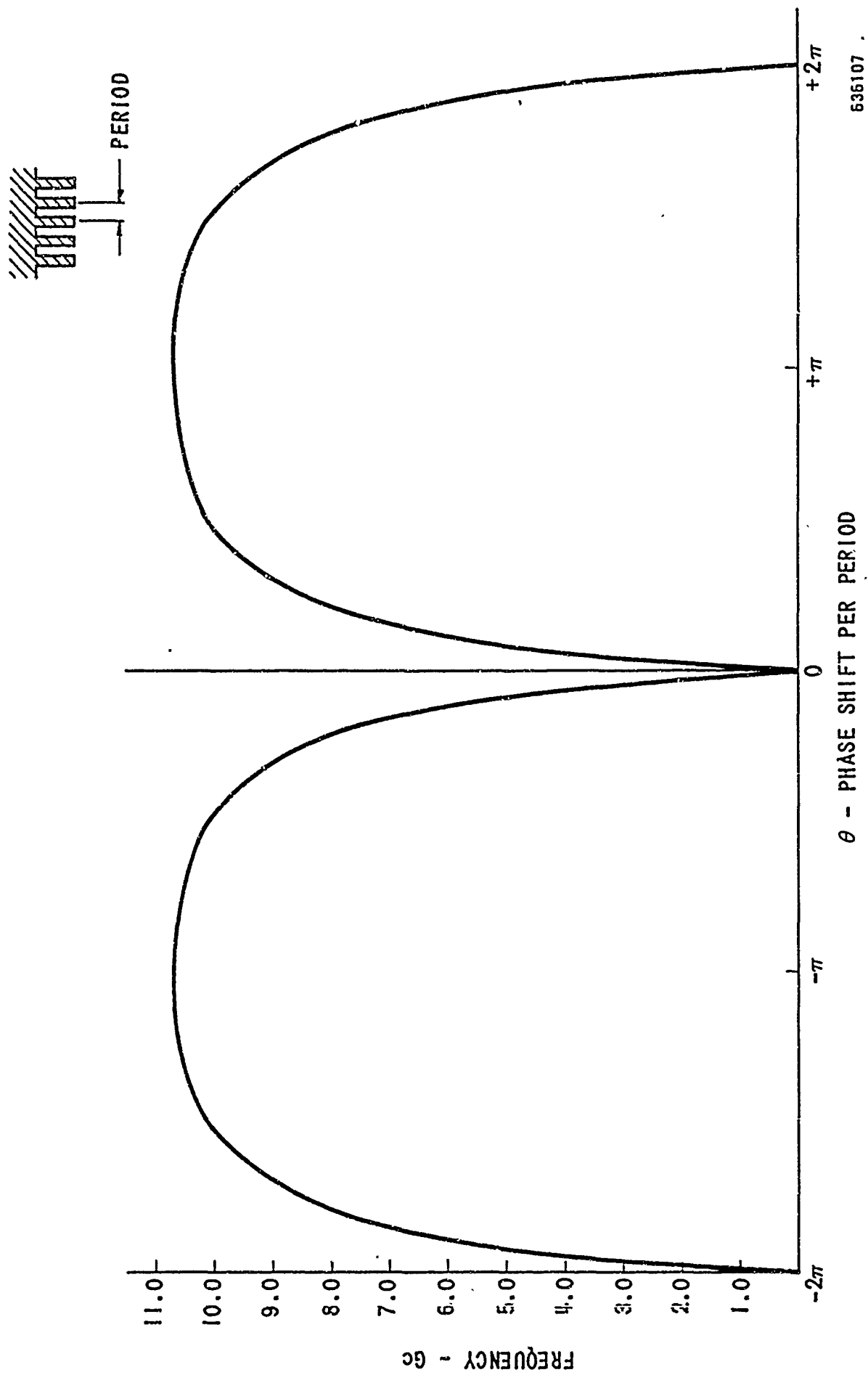|	Length (inches)	Width (inches)	Ratio of Slot to Vane Height	Ratio of Slot Width To Vane Gap
Slot I	0.335	0.0155	1.45	0.19
Slot II	0.424	0.017	1.84	0.21
Slot III	0.515	0.017	2.23	0.21

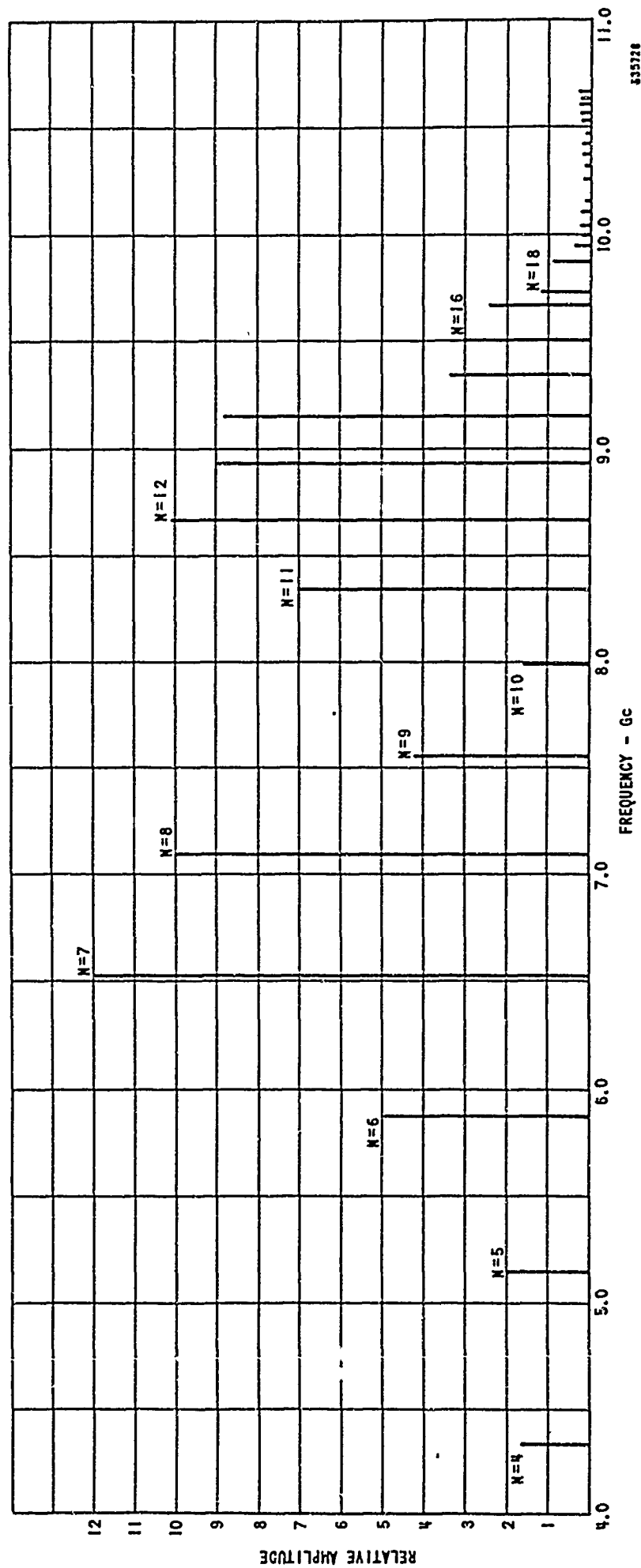FIGURE 3 $\omega - \beta$ Diagrem for Unslotted X-Band Anode

636107

Figure 4   Mode Spectrum Unslotted X-Band Anode

The mode patterns as determined in cold test for the three slotted anodes are given in Figures 5, 6, and 7. The relative amplitudes of the resonant frequencies are also shown. These mode spectra are characteristic of a bi-periodic structure with its two bandpass regions. A rising sun type magnetron has such a mode distribution. Therefore, the mode distribution of the multi-vaned coaxial magnetron can be considered similar to that of a modified rising sun magnetron. The rising sun magnetron consists of two sets of resonators in which alternate cavities have different depths. The resonant frequencies of the lower modes are determined primarily by the deeper resonators, while the resonances of the upper branch are associated with the shorter depth cavities. In the coaxial magnetron, alternate cells are coupled to the TE_{011} cavity by slots. These cells are analogous to the deeper resonators of the rising sun. Therefore, the slotted cells establish the resonant frequencies of the lower branch, while the resonances of the upper branch are linked to the unslotted anode cavities. It is observed from Figures 5 through 7 that X-band cold test information confirmed the modified rising sun description of the coaxial magnetron.

Figure 8, which illustrates the ω-β characteristic of the X-band anode with slot III, will be used to describe the mode distribution. The upper and lower branches of the spectrum are illustrated in this diagram. The circuit resonates at frequencies where the phase shift per period is given by

$$\theta = \frac{4\pi n}{N} \qquad \text{where } N = \text{Number of resonators}$$
$$n = 0, 1, 2, \ldots, \frac{N}{4}$$

Fast circuit TEM modes resonate at the lower frequencies of the bottom branch of the curve. Also, on this same branch, many resonances are clustered around the point of π phase shift per period (7.0 Gc). The normal π-mode operational point of a typical rising sun magnetron is shown to be at 8.25 Gc.
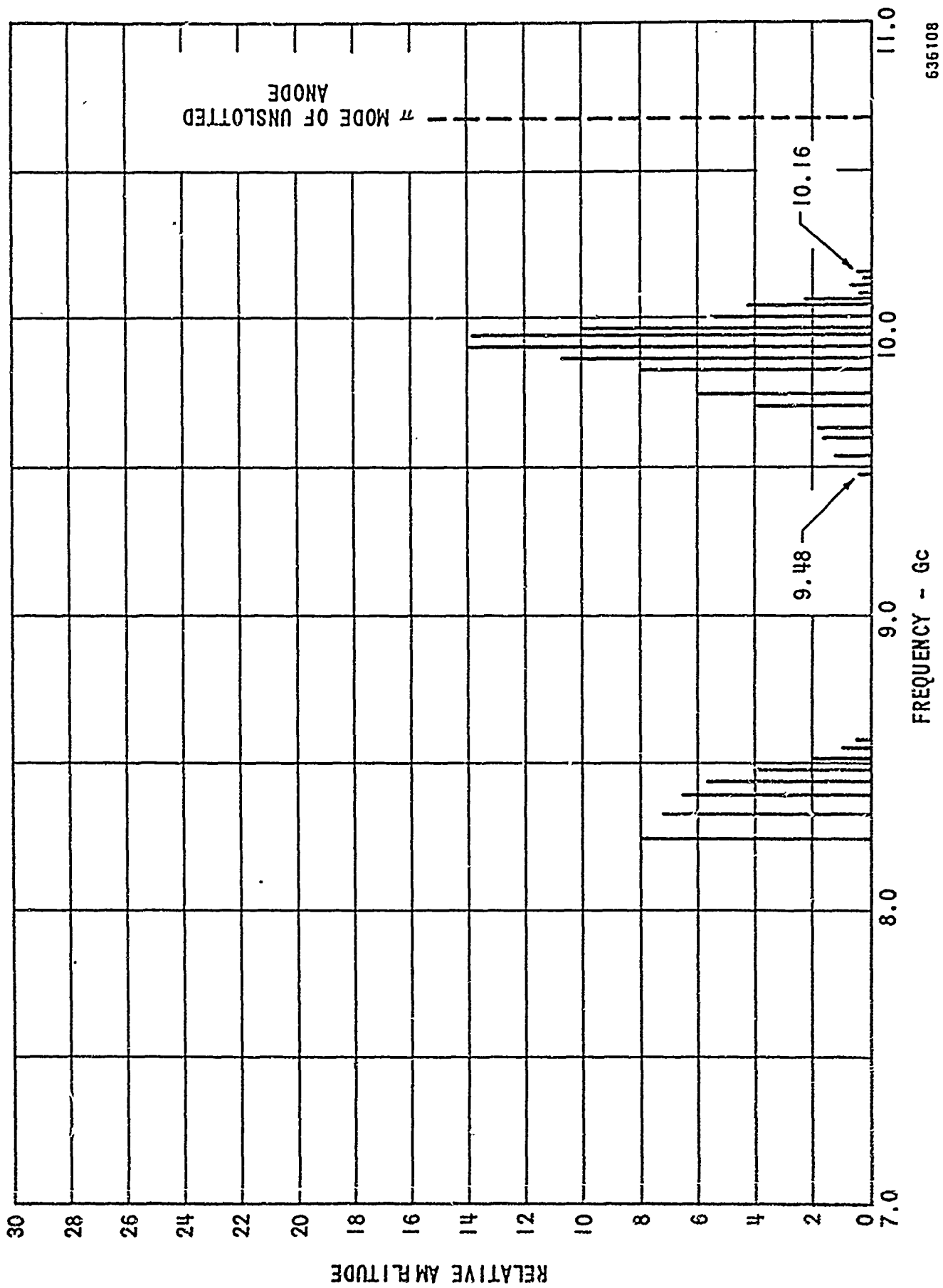
Figure 5 Mode Spectrum X-Band
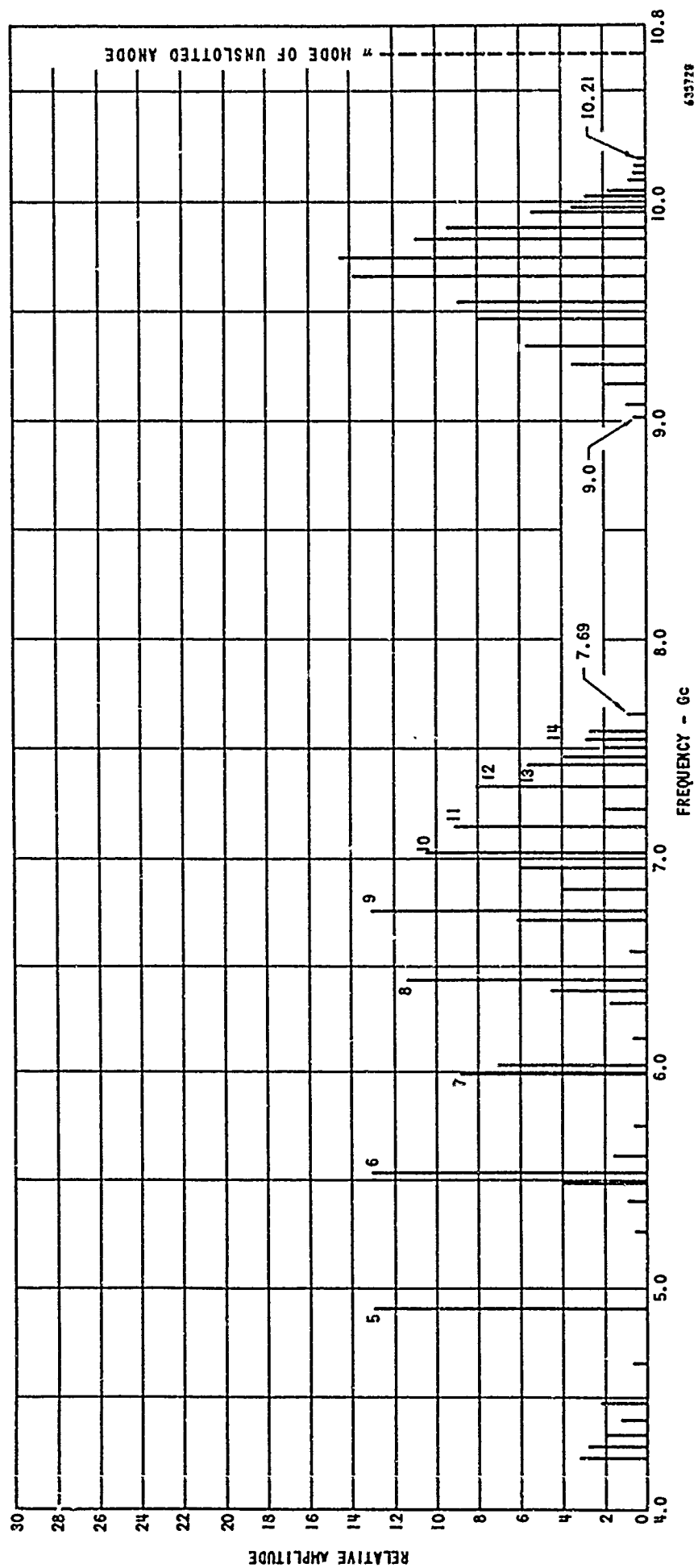Slot I L - .335"

636108

Figure 6   Mode Spectrum X-Band
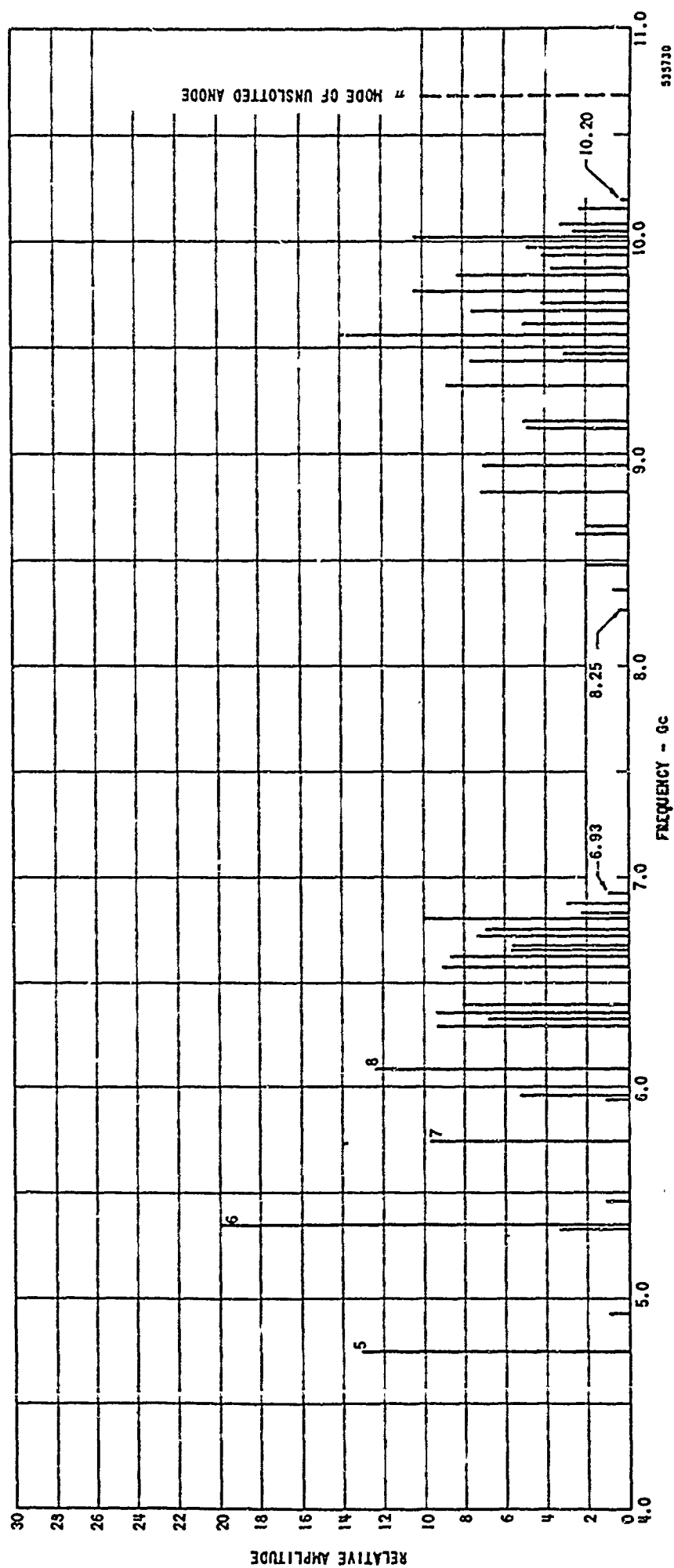Slot II   L - .424"
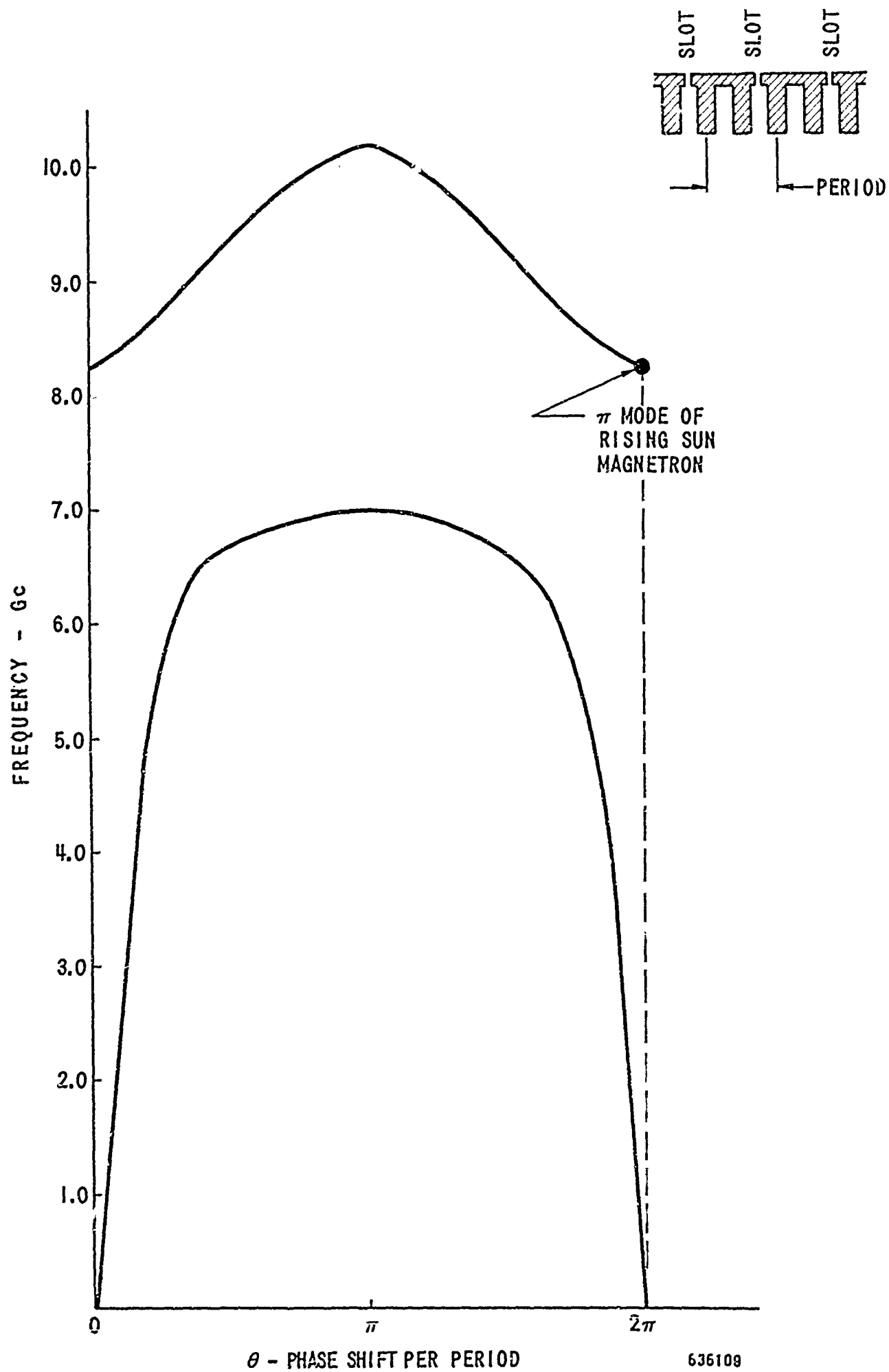
Figure 7 Mode Spectrum X–Band
Slot III L – .515"

FIGURE 8 $\omega - \beta$ Plot X-Band Anode with Slot
(.515" x .017")

From the analysis of the slotted multi-vaned anode, the upper cut-off frequency of the lower branch (π phase shift per period) occurred at the resonant frequency of the slotted resonator. Therefore, as the slots were elongated, this cut-off frequency became lower. Thus the slot length dimension was a means of controlling the frequency separation of the two branches. This separation corresponds to that obtained in a rising sun magnetron when the cavity depths are altered between the two sets of vanes. Figure 9 illustrates that the upper cut-off frequency of the lower branch is approximately linearly related to the slot depth. The separation between the two modes is plotted in the same figure. The upper and lower resonant frequencies of the upper branch are shown as functions of the slot lengths. Since the upper resonant frequency remained almost constant, it can be considered that it was associated with the unslotted cavities. Thus, the cold test results appear consistent with the modified rising sun model description of a multi-vaned coaxial magnetron. The information presented here will be employed in further description of the coaxial magnetron characteristics.

4.4.3 Slot Modes

From the analysis outlined in the previous section, all existing circuit modes can be accountable from the modified rising sun model. The circuit modes which present high interaction impedance to the electron beam are the so-called slot modes. Again using Figure 8, the slot modes for the X-band anode (slot III) were at 6.93 and 8.25 Gc. The phase shift per period for the circuit is π radians for 6.93 Gc while the 8.25 Gc resonance has 2π phase shift per period (π mode operational point of the conventional rising sun magnetron). The ω-β characteristic for the V-band anode, as obtained by scaling the phase diagram of the X-band anode, is shown in Figure 10.

Using this plot, the two slot modes scale to 63.75 Gc ($\theta = \pi$) and 75.9 Gc ($\theta = 2\pi$).
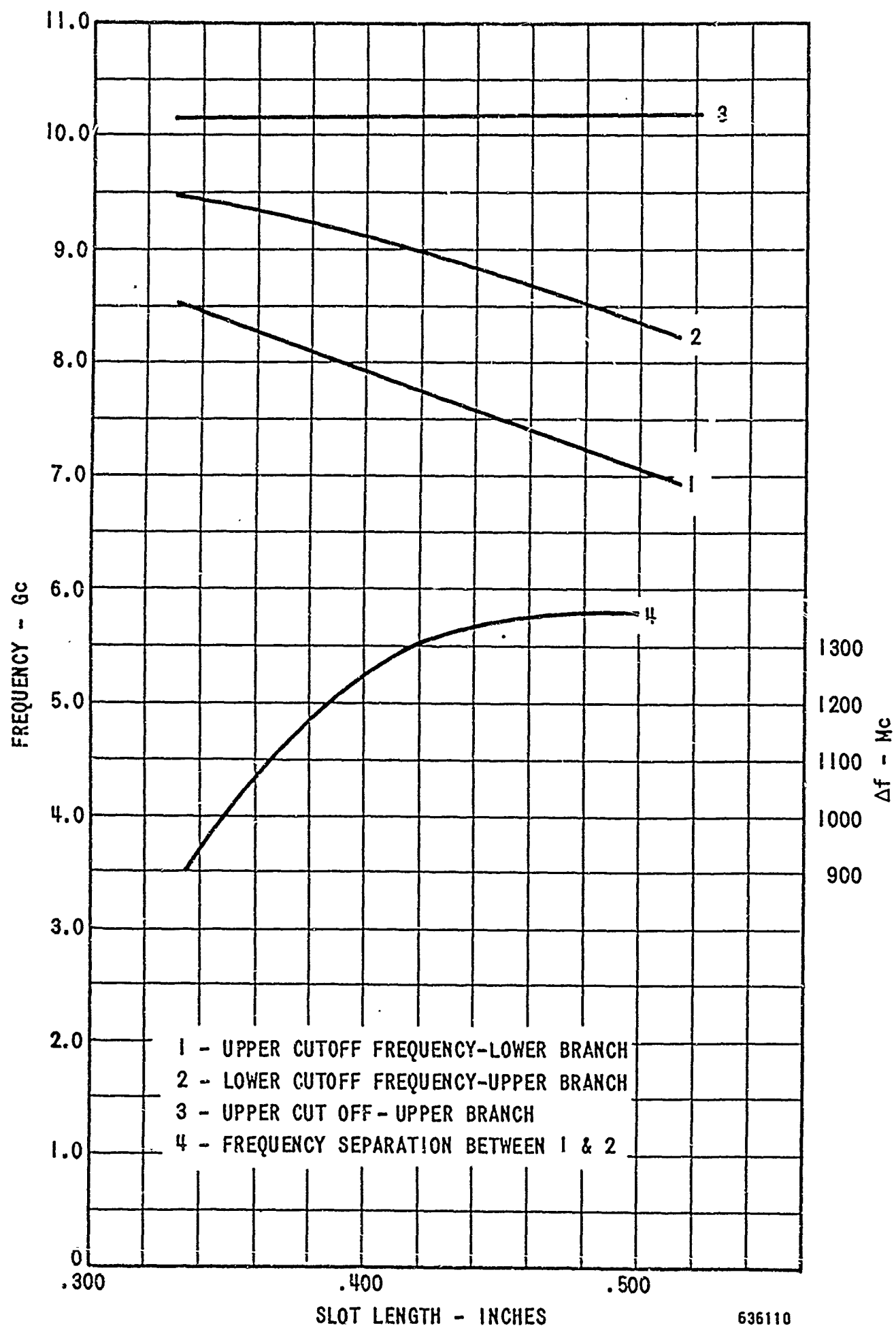
FIGURE 9 Slotted X-Band Anode
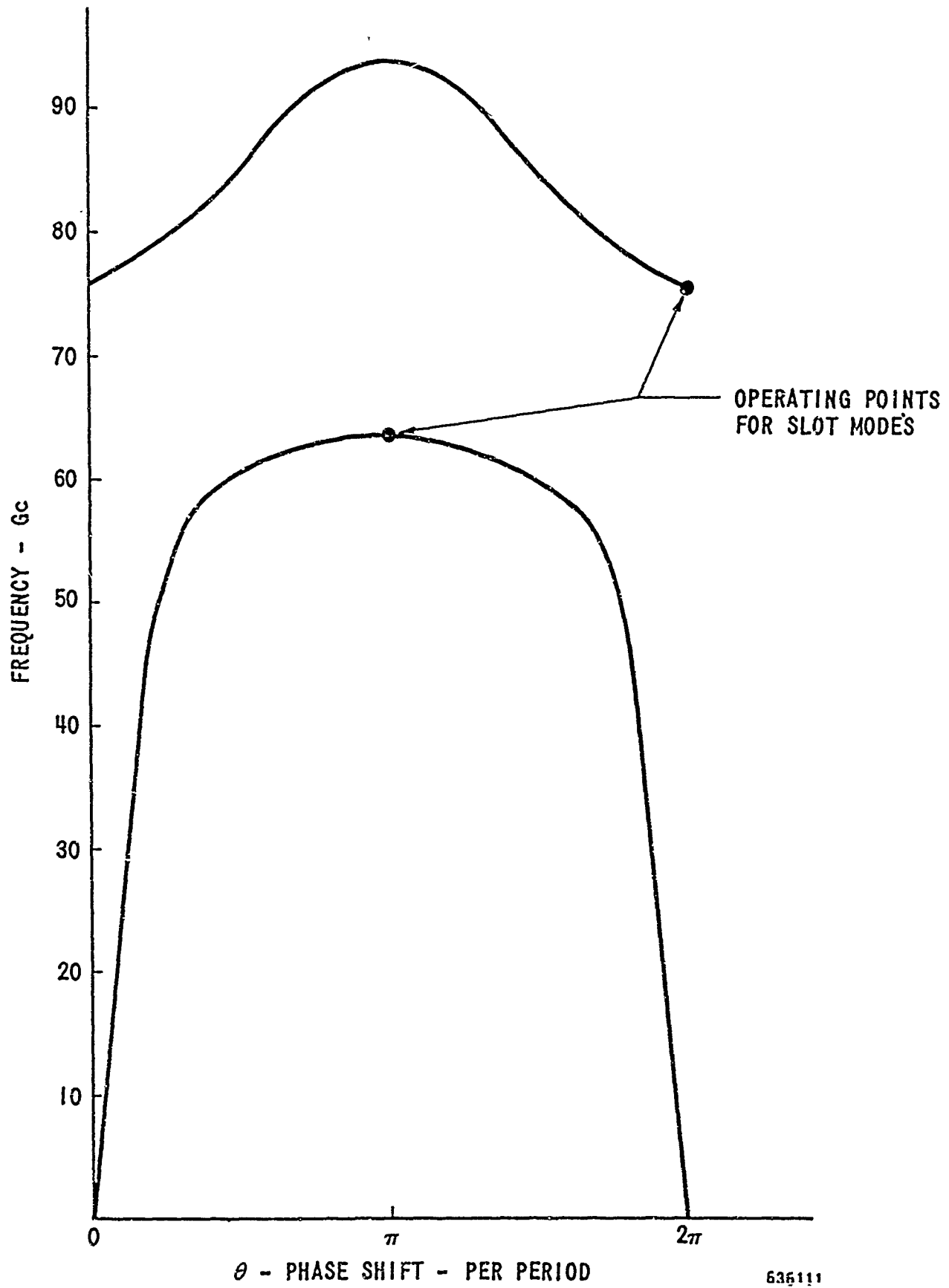Limiting Band Pass Frequencies

FIGURE 10 ω-β Diagram for V-Band Anode

The 75.9 Gc ($\theta \simeq 2\pi$) slot mode is the one that presents the more serious interference problem to normal operation. At a magnetic field of 20 kilogauss, the synchronous voltage for the π-slot mode is 16.4 KV, while 12.5 KV is the synchronous voltage for the 2π-slot mode. The synchronous voltage for the cavity-controlled 93.75 Gc mode of operation is 14.4 KV. Since the synchronous voltage of the 2π-slot mode is below that same voltage for 93.75 Gc operation, it is troublesome. The anode dampere should attenuate this 2π-slot mode.

Also one can consider the slot as a section of TE_{01} rectangular waveguide and compute its cutoff resonances. The final dimensions of the coupling slots of the scaled V-band anode were 0.056 inch x 0.002 inch. Hence, the computed resonant frequency for this slot was 105 Gc. This frequency is above that of the operational frequency and therefore should not present any interference to the TE_{01} oscillation.

4.4.4 Attenuation of Unwanted Modes

This part of the X-band cold test work was carried out with the purpose of developing a means of dampening the unwanted modes. The unwanted circuit modes consist of the anode circuit modes which include the slot modes as well as cavity and any other extraneous modes. Also, the program was directed towards the determination of the location and physical size of the damper.

Early cold-test work was performed to determine the effects of damper rings on the circuit modes of the unslotted and slotted I (0.335 inch x 0.0155 inch) anode. Since the unslotted anode and cathode structure

supports only vane mode resonances, the effectiveness of the damper rings on the attenuation of vane modes can be established without the interference of other modes.

Two damper rings were used in these cold tests: the rings were located on the output side of the outer anode wall. Damper ring I had a slide fit between the outer anode cylinder and the inner wall, while damper ring II had a 0.005-inch clearance between the same dimensions (V-band = 0.00055 inch). It was found for the two anode designs that damper ring I was far more efficient in attenuating the undesired circuit modes.

Again, the cold test data on the X-band model with slots I (0.335-inch x 0.017 inch) reaffirmed that damper ring I had considerably greater dampening effects than ring II. Thus, the location and dimensions of the damper appeared critical. It was observed that the lower order modes were strongly attenuated while the higher order modes were not as strongly dampened, with the exception of the modes which were in the neighborhood of the π-m⌐   For this reason, it appeared that the slot length was not optimum fo   elective loading of the modes.

The same experiments were performed on the anodes with slots II (0.424 inch x 0.017 inch) and slots III (0.515 inch x 0.017 inch). The relative attenuation of the various modes for the anode with slots II is shown in Figure 11, while Figure 12 indicates the relative attenuation of the circuit modes for the anode with slots III and dampers I and II for various axial positions of the damper. The anode vane faces were the reference zero plane for axial positions. Again, these data showed that the circuit modes were effectively attenuated by the damper with the press fit between the anode and cylinder. Thus, it is essential that the damper at V-band be in close proximity to the anode under all operating conditions for satisfactory attenuation of the desired modes. The information presented in Figures 11 and 12 was used in designing the V-band damper. By elongating the slots, the coupling between the cavity and anode increased. It was also thought that longer slots would allow the damper to be placed further away from the anode vanes and still be as effective in suppression of the undesired modes. The further the damper was situated from the vanes, the higher the unloaded Q's. From cold test results (Figures 13 and 14), the attenuation of the damper on the circuit modes was found to be fairly independent of the coupling slot length. The attenuation of the circuit modes depended almost entirely on the location and contact of the damper with respect to the anode. The relationship of the damper location with respect to the unloaded Q of the system will be discussed in the next section.

4.4.5 Coupling of the Coaxial Magnetron to the Output

The anode is coupled by slots to the TE_{011} coaxial cavity, which, in turn, is coupled to the TE_{01} circular waveguide. The amount of coupling between the anode and cavity is established by the size of the coupling slots. The coupling between the cavity and output is controlled by the cavity plate. Thus, the degree of coupling is adjusted by the diameter of this plate.
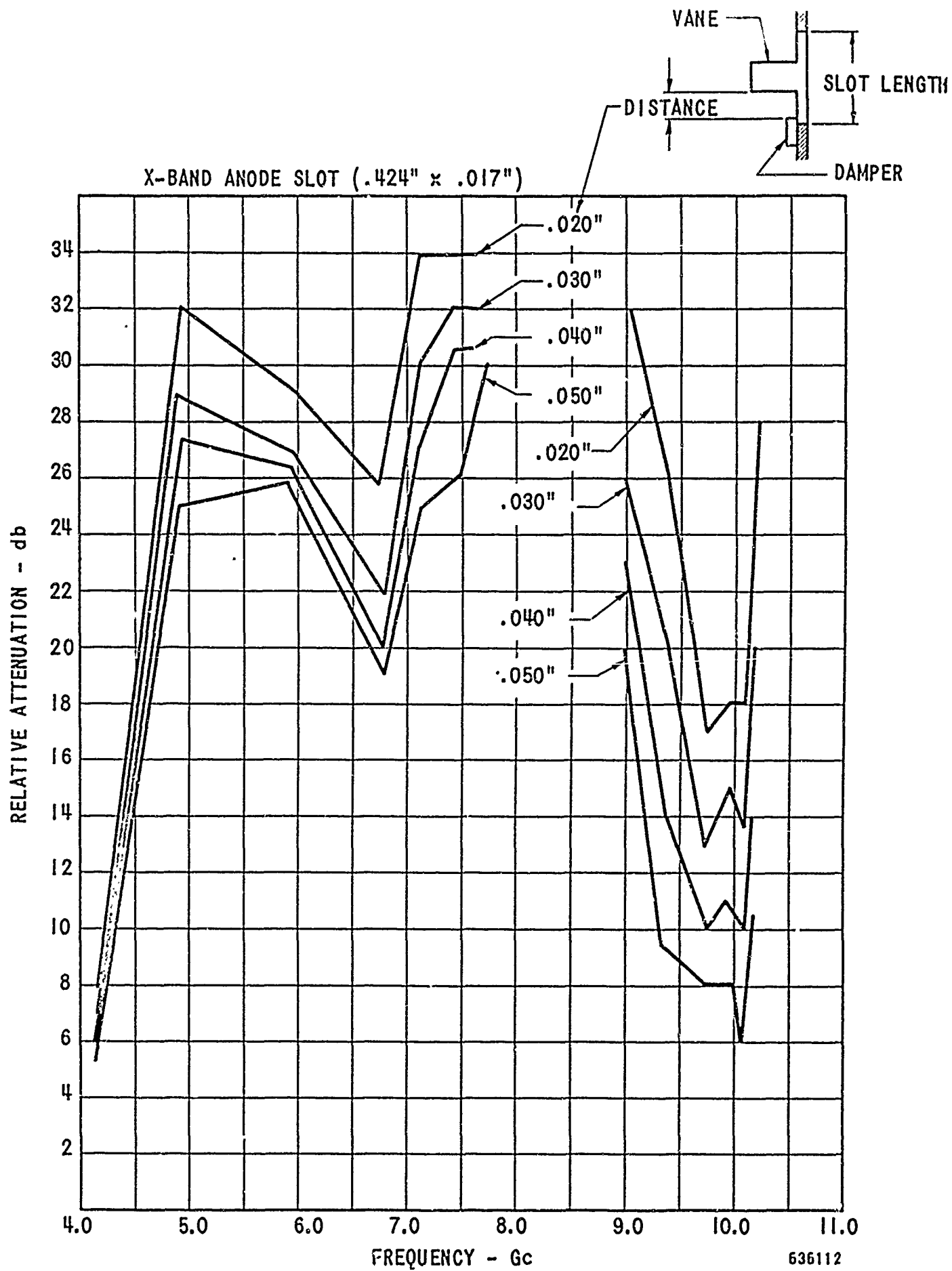
FIGURE 11   Relative Attenuation of X-Band Circuit Modes
for Axial Position of Damper I
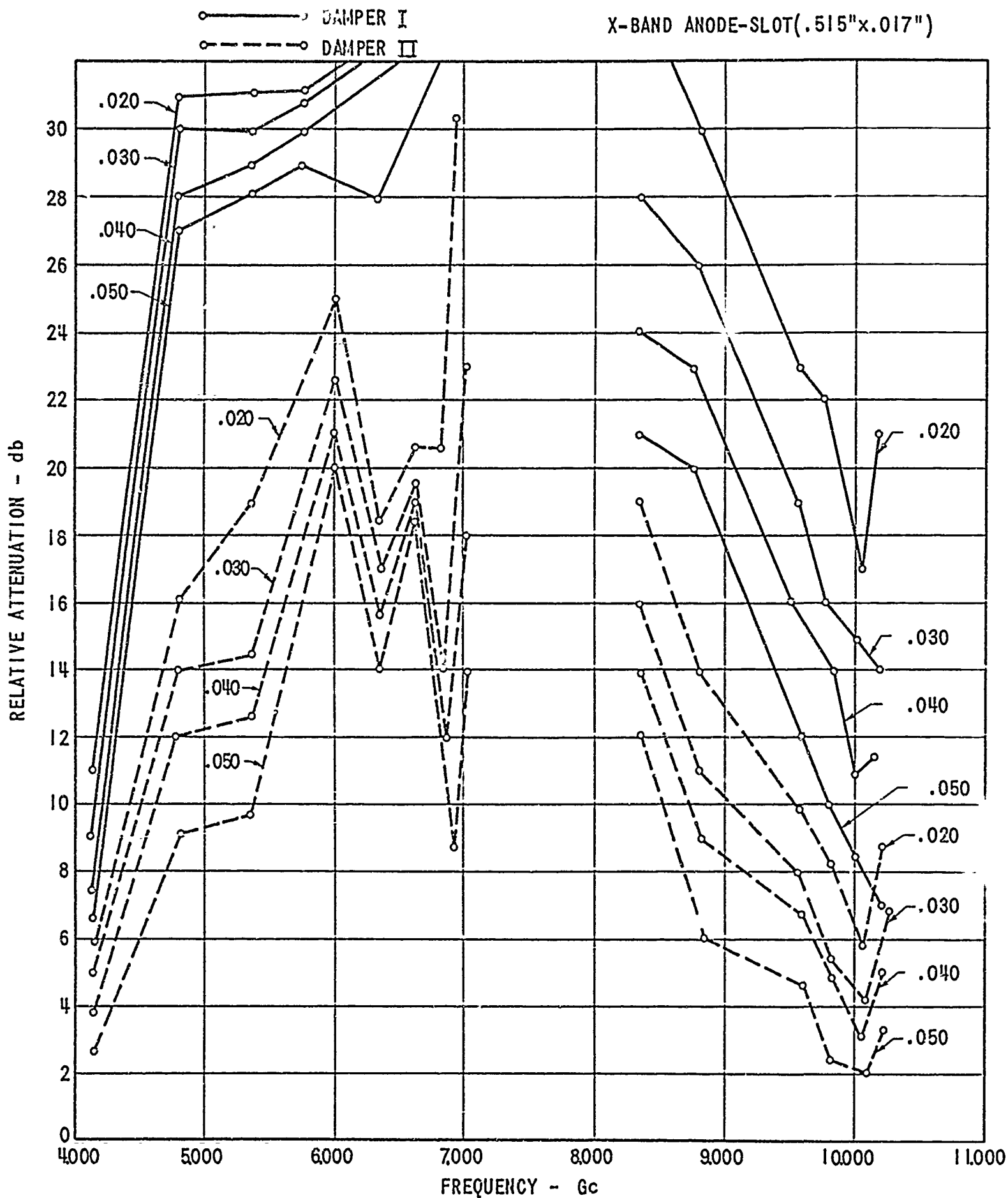
FIGURE 12   Attenuation of Circuit Modes for
Axial Position of Dampers I and II
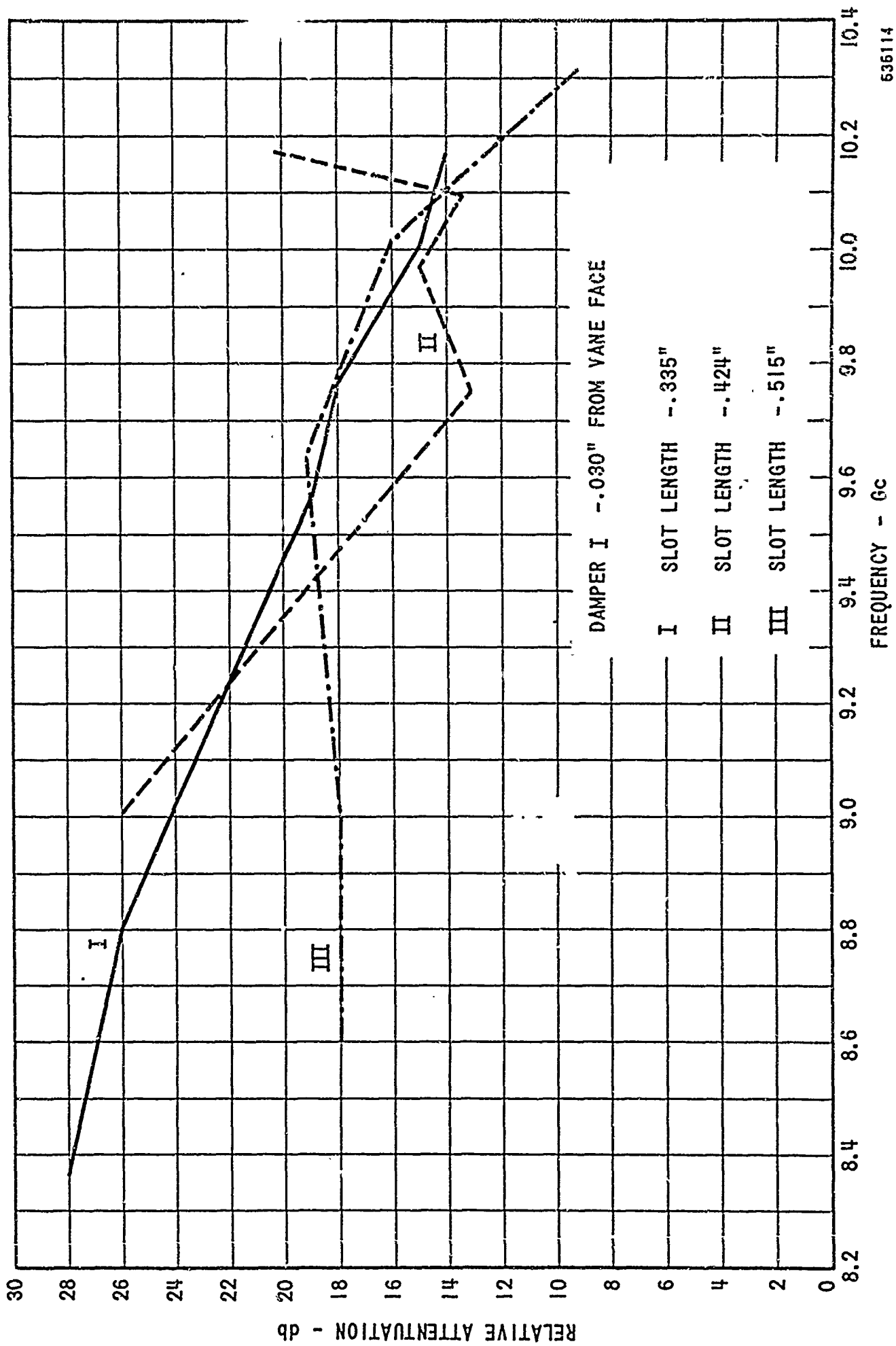
FIGURE 13 Attenuation of the Upper Modes - X-Band Anode

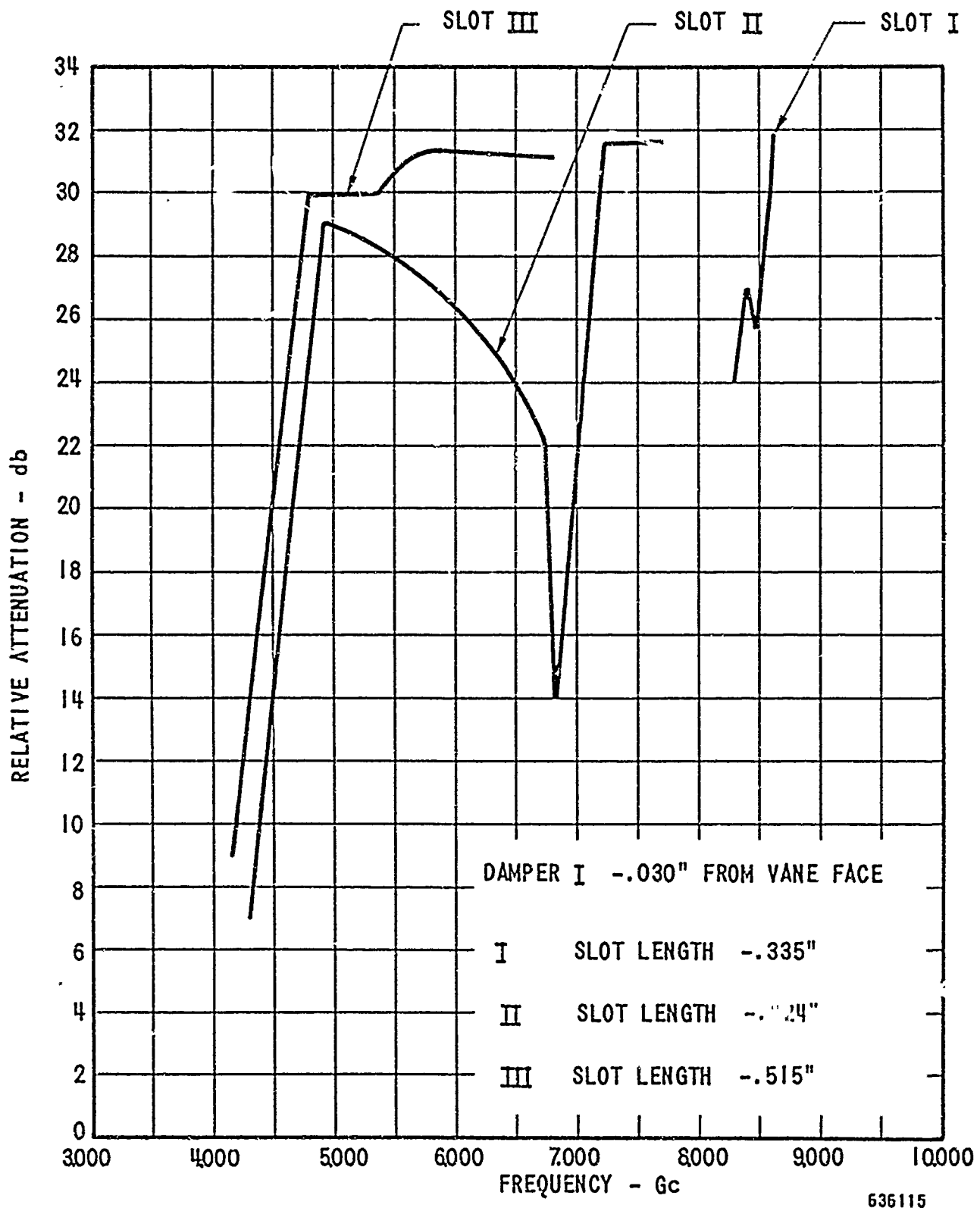Y-axis: RELATIVE ATTENTUATION - db

X-axis: FREQUENCY - Gc

DAMPER I -.030" FROM VANE FACE

I   SLOT LENGTH -.335"

II   SLOT LENGTH -.424"

III SLOT LENGTH -.515"

536114

FIGURE 14   Attenuation of Lower Modes – X-Band Anode

- 28 -

This type of output coupling has several distinct advantages. It tends to load down other cavity modes. The 3 cavity resonances which are in the vicinity of the TE_{011} mode are the TE_{311}, TE_{211} and TM_{111} (degenerate with the TE_{011}). Also, the power handling capabilities of the circular TE_{01} waveguide is considerably greater than a corresponding TE_{10} rectangular waveguide. Finally, the mechanical features of the circular TE_{01} waveguide are simpler than those of the rectangular waveguide.

The parameter, Q_E, is a measure of the coupling of the tube to the external load. Besides output power considerations, electronic efficiency and stabilization enter into the determination of the Q_E of the coaxial magnetron. With low Q_E, the rf voltage is weak in the interaction space. Hence, there is a lower efficiency for conversion of dc power to rf power. However, if the Q_E is too high, stabilization problems will arise. These problems will be manifested by misfiring and starting troubles. The desired external loading can be more precisely determined from hot test results. Table V indicates the Q_E and Q_L measured for different iris diameters. This information will be utilized in designing the output coupling scheme for the V-band tube.

TABLE V

MEASURED EXTERNAL AND LOADED Q'S

a. Q_L (Slotted III - X-band anode)

	Iris Dia (inches)			
f(Gc)	1.200	1.250	1.300	1.350
10.1	1010	1490	1840	1450
10.22	1990	2920	3170	3170
10.40	1780	2510	3500	4500
10.53	928	1360	1820	2120
10.72	832	980	828	465

TABLE V (Continued)

b. Q_E (Slotted III - X-band Anode)

f(Gc)	Iris Dia (inches)			
	1.200	1.250	1.300	1.350
10.1	1830	3580	7000	9800
10.22	4720	9000	20000	38000
10.40	2780	5020	11200	38500
10.53	1300	2500	4800	11000
10.72	1670	2350	3800	3050

Desirable target values for the Q's for the V-band tube are

$$Q_L = 475 \quad \text{where} \quad Q_L = \text{Loaded Q}$$

$$Q_U = 1200 \quad\quad\quad\quad Q_U = \text{Unloaded Q}$$

$$Q_E = 790 \quad\quad\quad\quad Q_E = \text{External Q}$$

In examining the effects of the iris dimensions on the unloaded Q, it was noticed that the unloaded Q could be optimized through the selection of the proper iris diameter. This observation will be discussed in the next section.

4.4.6   The Unloaded Q

The unloaded Q of the coaxial magnetron is an important design parameter. The coaxial magnetron possesses an unloaded Q which is considerably higher than those of a conventional magnetron for a corresponding resonant frequency. Because of this higher unloaded Q, the coaxial magnetron has more stable operation at higher efficiencies. Also, the coaxial magnetron has a wider tuning range than a conventional magnetron. The theoretical Q of the TE_{011} cavity is at least double that of other common mode cavities. The high Q results from the fact that the current paths are purely circumferential for this mode. This feature permits the tuning range to be achieved by a simplified tuner.

The unloaded Q's of the first unslotted X-band cavity are plotted in Figure 15. These Q's were well below the theoretical values. As the slot lengths are increased, the coupling between the cavity and anode becomes tighter. Also, the unloaded Q decreases with the longer slots because of slot radiation. Therefore, since the tight coupling between the anode and cavity is accomplished at the expense of lower unloaded Q's, the selection of slot length will be a compromise between these two parameters. In Figure 16, the influence of slots on unloaded Q's is illustrated. It is noticed from these data that the losses increase fairly sharply with the longer slots. As mentioned, these losses will dictate the amount of coupling that can be acceptable between the cavity and anode.

Another loss which enters and further reduces the unloaded Q comes from the anode damper. As the undesired circuit modes are suppressed by placing the damper closer to the anode vanes, the damper losses enter into the unloaded Q's. Figure 17 illustrates these results.

Also, the relationship of the resonant frequency of the TE_{011} cavity to the circuit modes plays an important role in the unloaded Q's. If the cavity is tuned to a frequency where the circuit modes exist, the unloaded Q's are very poor. These losses are due to radiation from the vanes. The best unloaded Q's were found to be at the π-mode frequency of the unslotted anode.

Next, it was found that the coupling iris influenced the unloaded Q's. The unloaded Q's for the X-band model for various coupling iris diameters are shown in Table VI.
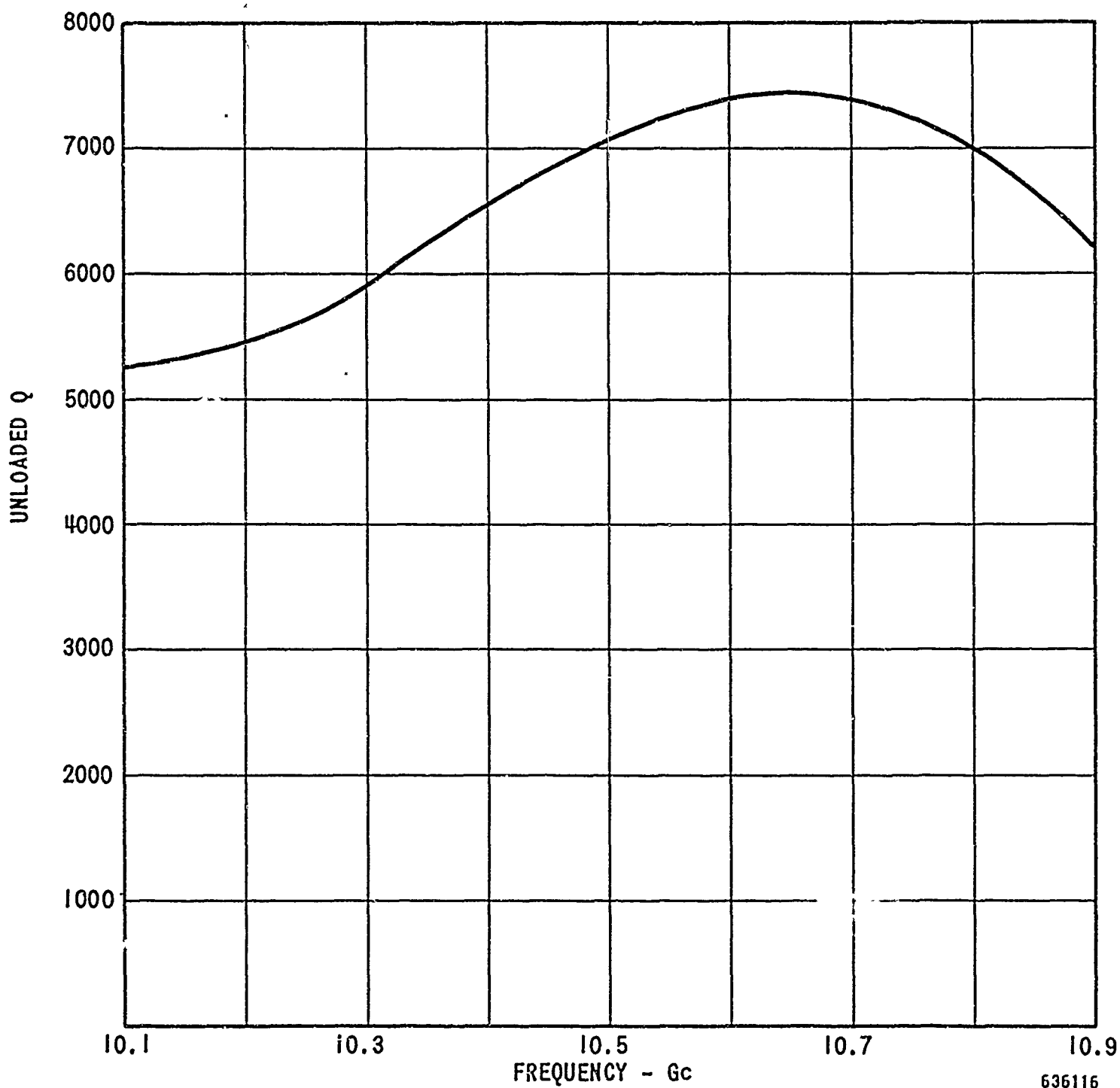
FIGURE 15   Unslotted X-Band Anode
Unloaded $Q - TE_{011}$ Mode
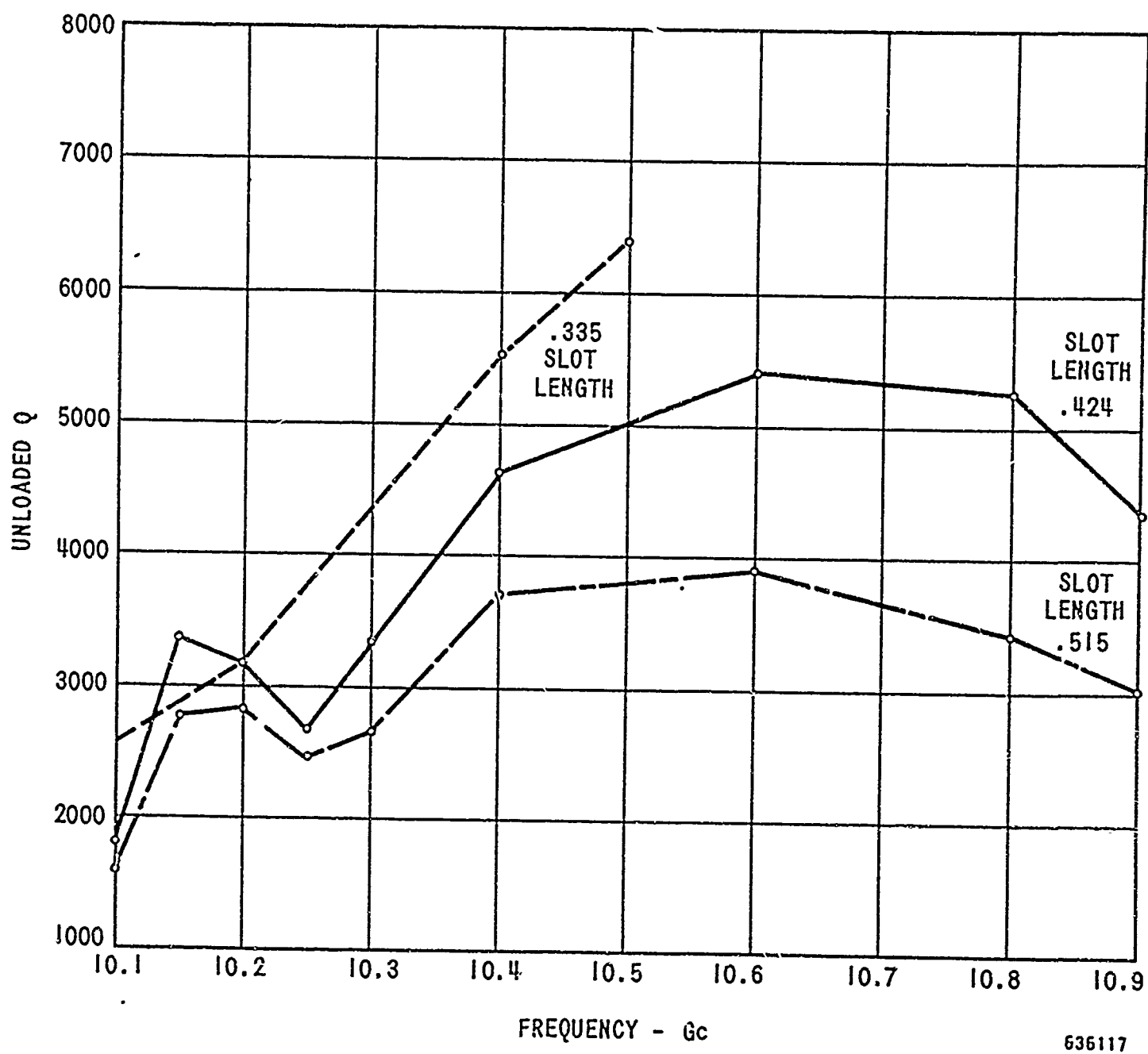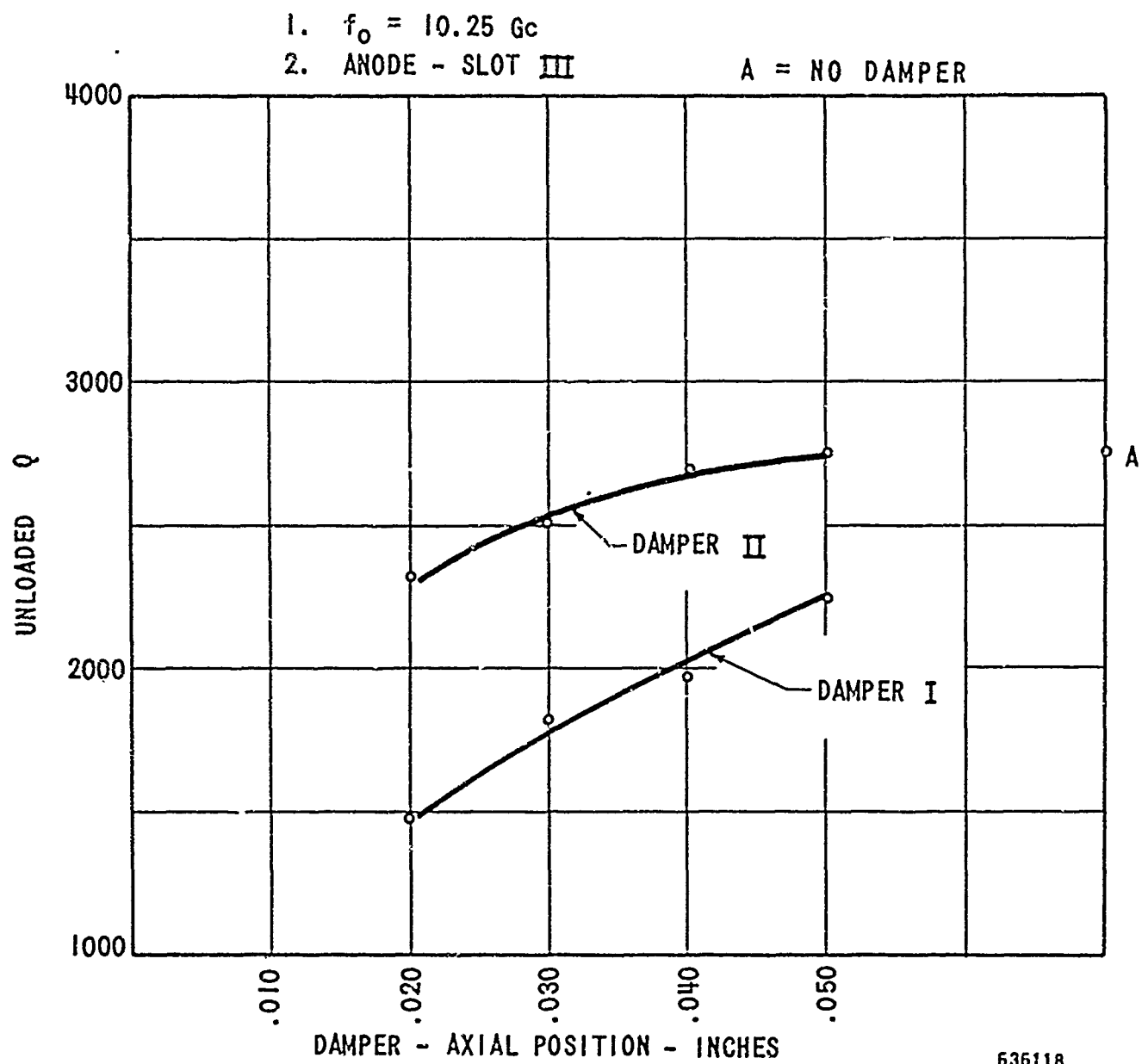
FIGURE 16   Unloaded Q – Slot Length
(no damper)

FIGURE 17   Unloaded Q – Dampers I and II

TABLE VI
UNLOADED Q'S OF X-BAND MODEL

	Iris Dia (inches)			
f(Gc)	1.200	1.250	1.300	1.350
10.10	2250	4020	2500	1730
10.22	3560	2630	3820	3480
10.40	5000	5020	5010	5000
10.53	3100	3020	2880	2600
10.72	1670	1910	1060	565

Since the unloaded Q's were generally lower than expected, efforts were made to improve them. First, the center conductor was plated to reduce cavity surface losses. Also, a small groove was machined into the base of the cavity. This groove acts as a perturbation which decouples the TM_{111} and TE_{011} modes. These two factors had a significant effect on improving the unloaded Q. The unloaded Q's for the unslotted cavity with these two features are given in Figure 18, while unloaded Q's for the slotted anode-cavity (0.515 inch x 0.017 inch) are plotted in Figure 19. Further cold test work proved that the unloaded Q could be made even higher by selective loading.

4.4.7 Cavity Modes

The 2 cavity resonances that appear closest to the TE_{011} mode are the TE_{211} and TE_{311} modes. These 2 modes do not couple as readily to the anode circuit as the TE_{011} mode. In addition, both modes are suppressed by the loading down effects of the coupling iris and anode damper. The attenuation of the TE_{211} and TE_{311} due to the anode damper is shown in Table VII.
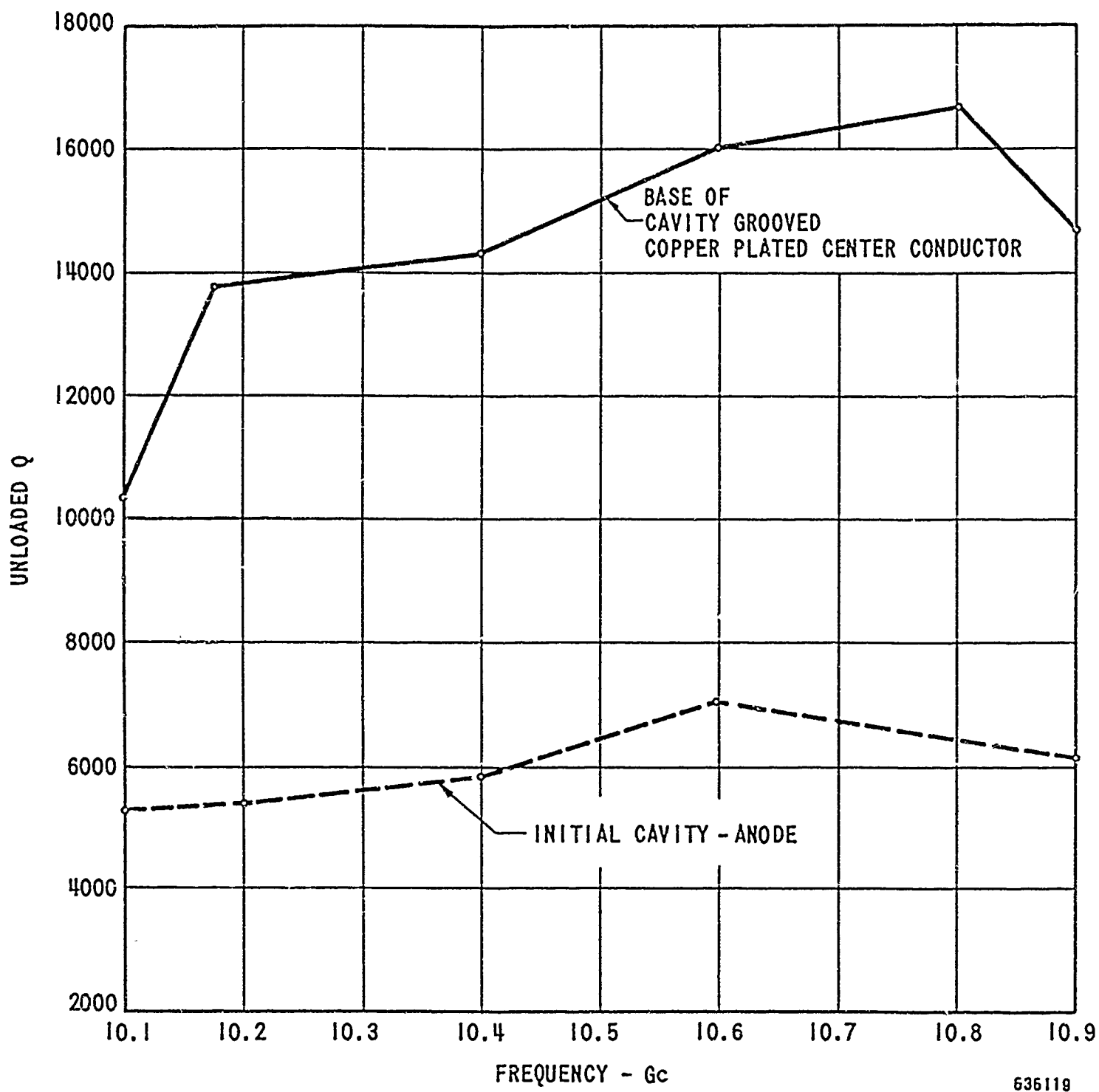
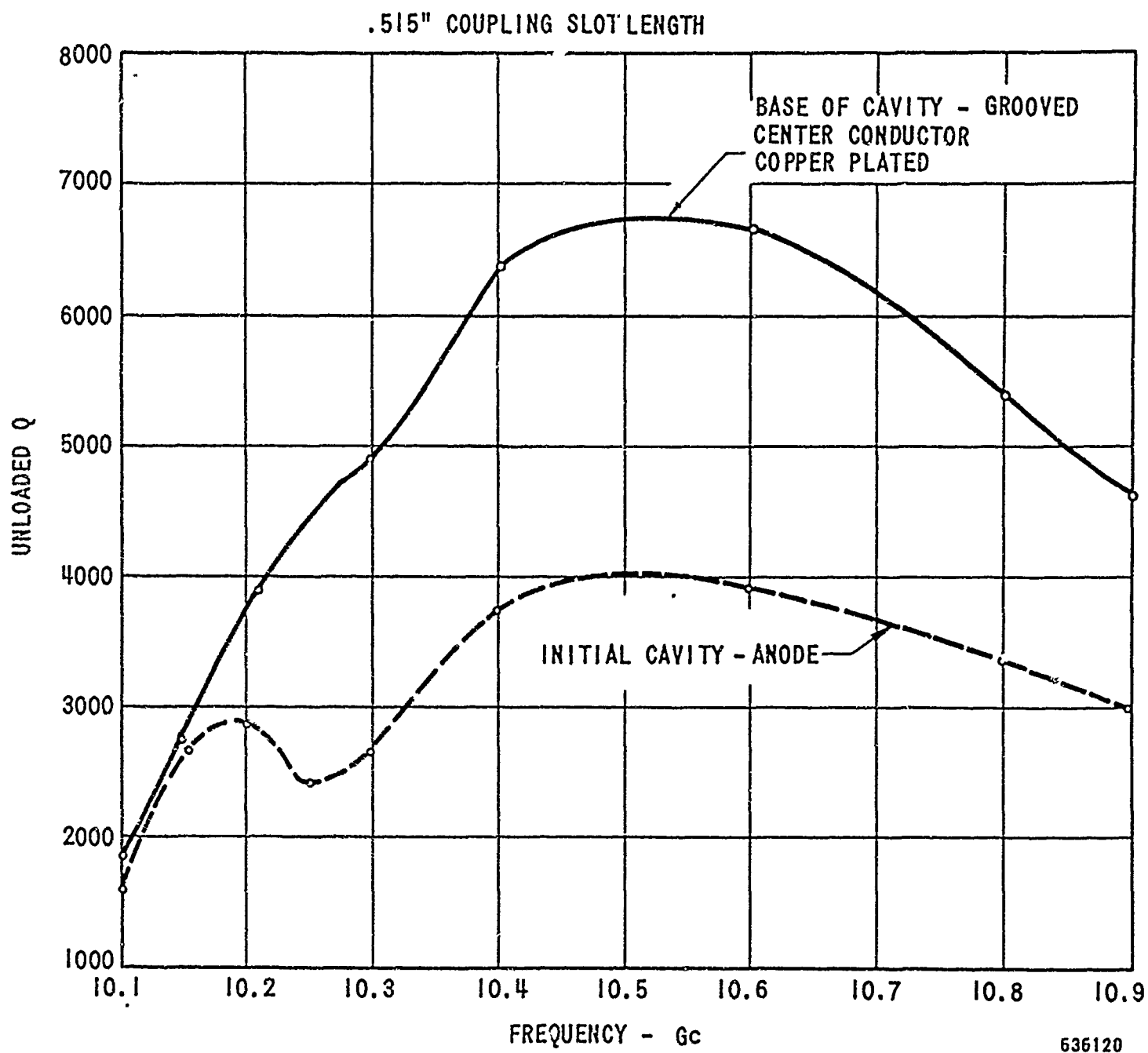FIGURE 18   Unloaded Q - Conventional TE_{011} Cavity
(not slotted)

.515" COUPLING SLOT LENGTH

FIGURE 19   Unloaded Q – Conventional TE$_{011}$ Cavity
(Slotted)

TABLE VII

ATTENUATION DUE TO ANODE DAMPER

a. TE_{211} (TE_{011} set at 10,630 Mc)

f_2(Mc)	Q_{U2}	Remarks
9218	7850	Unslotted anode
9218	1685	0.515 inch slotted anode; no damper
9218	1350	0.515 inch slotted anode; damper at 0.150 inch
9218	1180	0.515 inch slotted anode; damper at 0.100 inch
9218	745	0.515 inch slotted anode; damper at 0.050 inch
9218	592	0.515 inch slotted anode; damper at 0.030 inch

b. TE_{311} (TE_{011} mode at 10,450 Mc)

f(Mc)	Q_U	Remarks
11,210	2850	Unslotted anode
11,210	1990	0.515 inch slotted anode, no damper
11,210	1930	0.515 inch slotted anode; damper at 0.150 inch
11,210	1490	0.515 inch slotted anode; damper at 0.100 inch
11,210	Very heavily loaded	0.515 inch slotted anode; damper at 0.050 inch

The TM_{111} mode is degenerate with respect to the TE_{011} cavity mode. The coupling iris removes this degeneracy as well as loading down the TM_{111} mode. Also, the addition of a small groove in the base of the cavity separates the two modes and appreciably raises the unloaded Q of the TE_{011} cavity mode. The tuning curves for the 3 transverse electric modes are plotted in Figure 20 for the X-band anode.
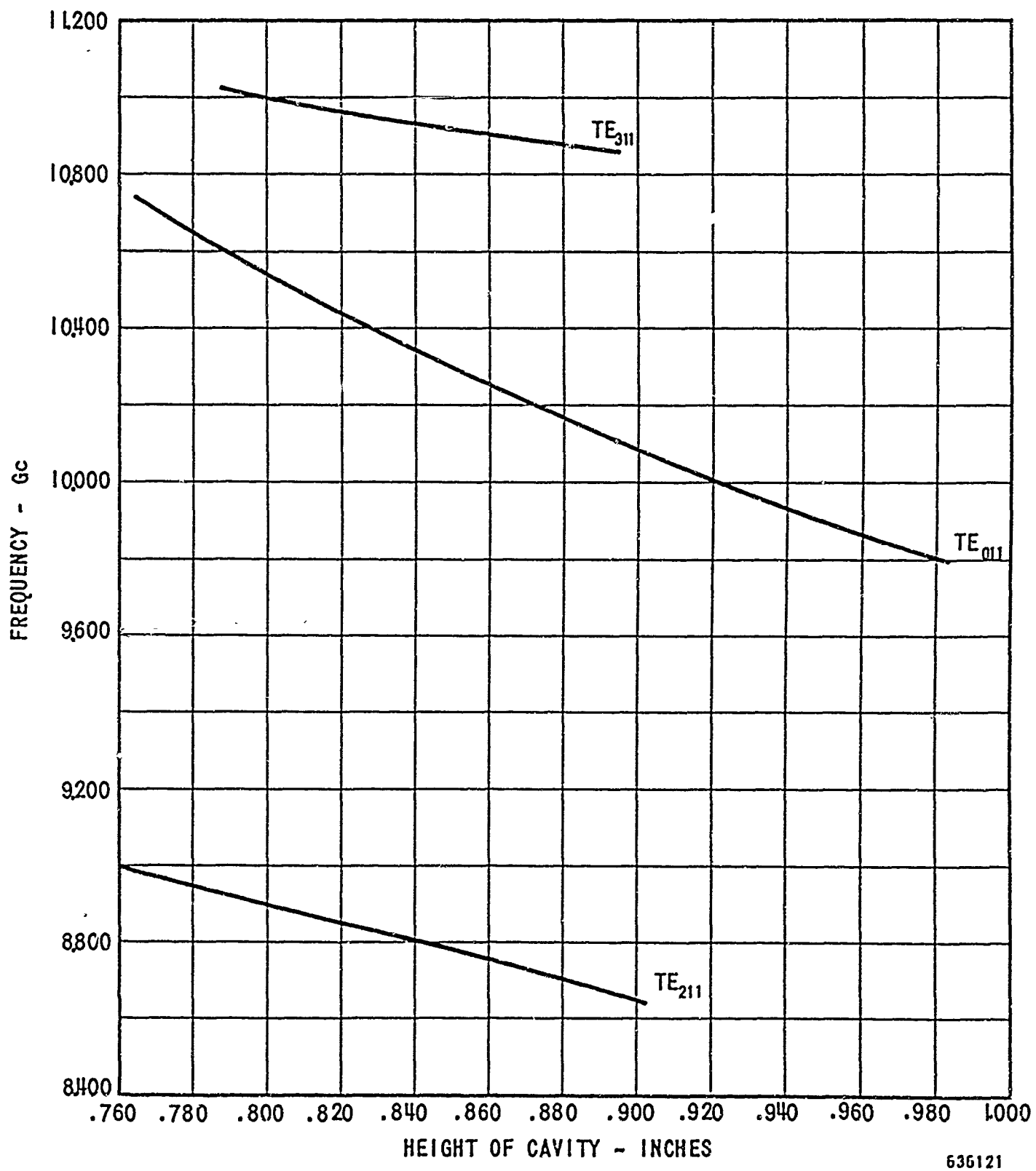
FIGURE 20   Tuning Curve X–Band Anode
Slotted (.515" x .017)

636121

4.4.8 Fast Cyclotron Mode Interaction

In a crossed-field device, 4 beam waves may be excited. These waves include both the fast and slow diocotron waves as well as the fast and slow cyclotron waves.

The wave propagation constant, β_1, for the fast cyclotron wave is given by

$$\beta_1 = \beta_e - \beta_c;$$

while the propagation constant, β_2, for the slow cyclotron wave is

$$\beta_2 = \beta_e + \beta_c,$$

where the electron phase constant, β_e, is

$$\beta_e = \frac{\omega}{v_o} \ .$$

v_o is the electron drift velocity and equals

$$\frac{\vec{E} \times \vec{B}}{B^2} \ .$$

The cyclotron phase constant, β_c, is given by:

$$\beta_c = \frac{\omega_c}{v_o} \ ,$$

where

$$\omega_c = 2\pi f_c$$

The cyclotron frequency in Gc is related to the magnetic field in kilogauss by

$$f_c = 2.8 \times B$$

In crossed-field millimeter tubes, the fast cyclotron mode inter-
action has been a problem. Raytheon has investigated this mode inter-
ference problem for millimeter carcinotrons. The reason the problem
arises in millimeter tubes is that the magnetic field is such that cyclotron
frequency lies below the operating frequency. In centimeter wavelength
magnetrons, the converse is true, i. e., the cyclotron frequency is higher
than the operational frequency.

Fast cyclotron interaction can occur in crossed-field devices when
the propagation constant of this mode corresponds to that of a circuit wave.
In Figure 21, the ω-β characteristic for the V-band tube, the fast cyclotron
wave propagation relationships are plotted for a magnetic field of 15 kilo-
gauss for various voltages. As the voltage increases, the slope of the
curve becomes greater. Where these propagation curves intersect the
phase curves of the anode, cyclotron interaction can take place. From this
figure, it can be seen that there are many regions for cyclotron interaction.

As mentioned in Section 4.4.2, Analysis of Multivane Coaxial
Structures, fast circuit waves exist for low frequency circuit resonances.
In these modes, the electric fields are present in the interaction space and
there are no transverse E fields across the vane gaps. While this field
configuration will yield a low interaction impedance for magnetron inter-
action, it can be high for cyclotron interaction. Also, the cyclotron inter-
ference can exist at frequencies corresponding to resonant frequencies of
the upper branch of the anode mode pattern. Here electric fields are strong
at the vane surfaces. Therefore, the anode damper should be somewhat
effective in controlling this cyclotron interaction.

There are several possible solutions in eliminating cyclotron inter-
ference at the low mode resonant frequencies of the circuit. First, for high
magnetic fields, the cyclotron frequency is greater than the highest fre-
quency of the lower mode; hence, no cyclotron reaction can result from the
interaction of the forward circuit waves with the fast cyclotron beam wave.
For the V-band model, this frequency is 63.75 Gc. Therefore, the magnetic
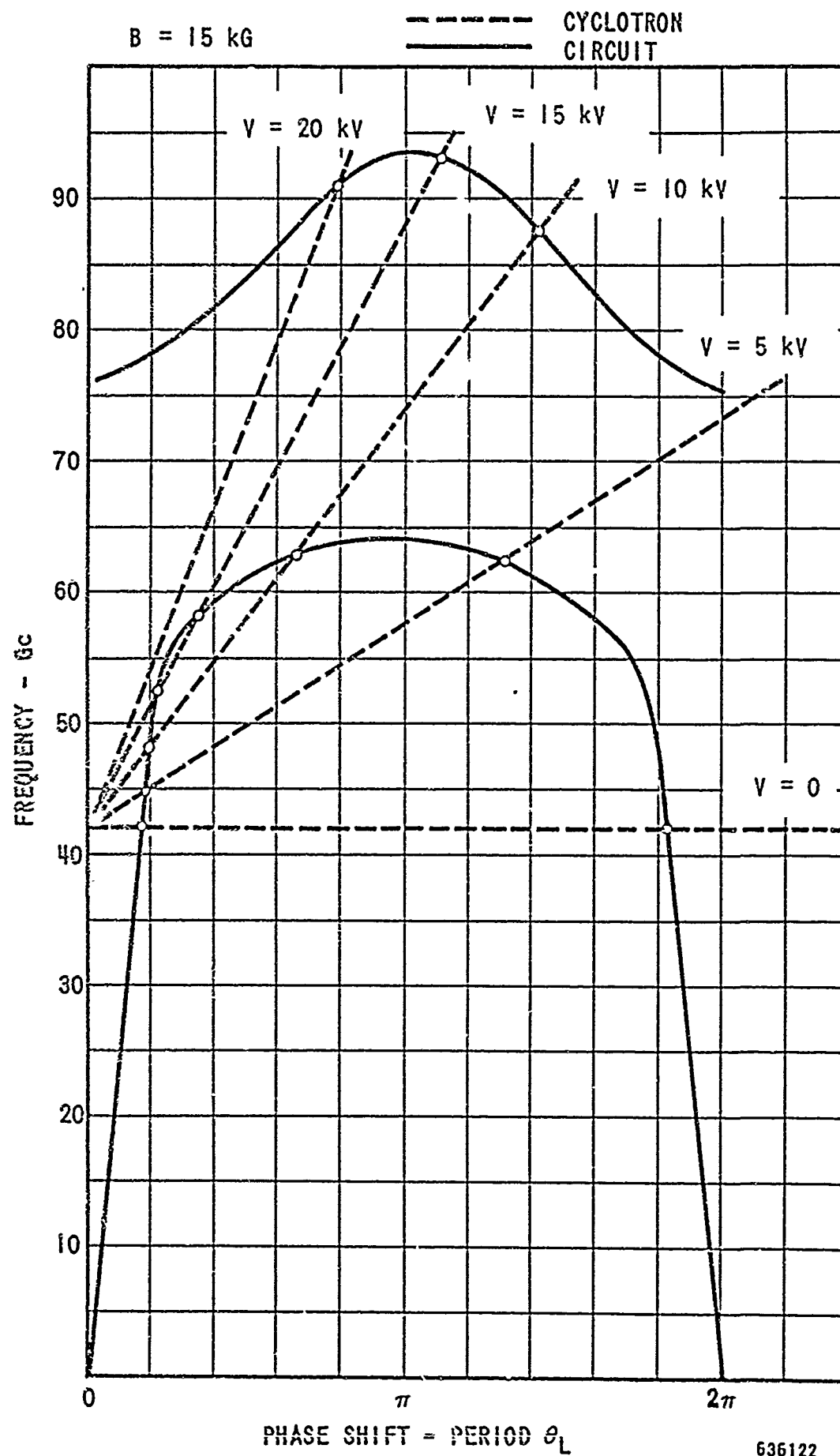field should be greater than 22.8 kilogauss. The upper frequency of the

FIGURE 21   V-Band - $\omega - \beta$ Diagram with Fast
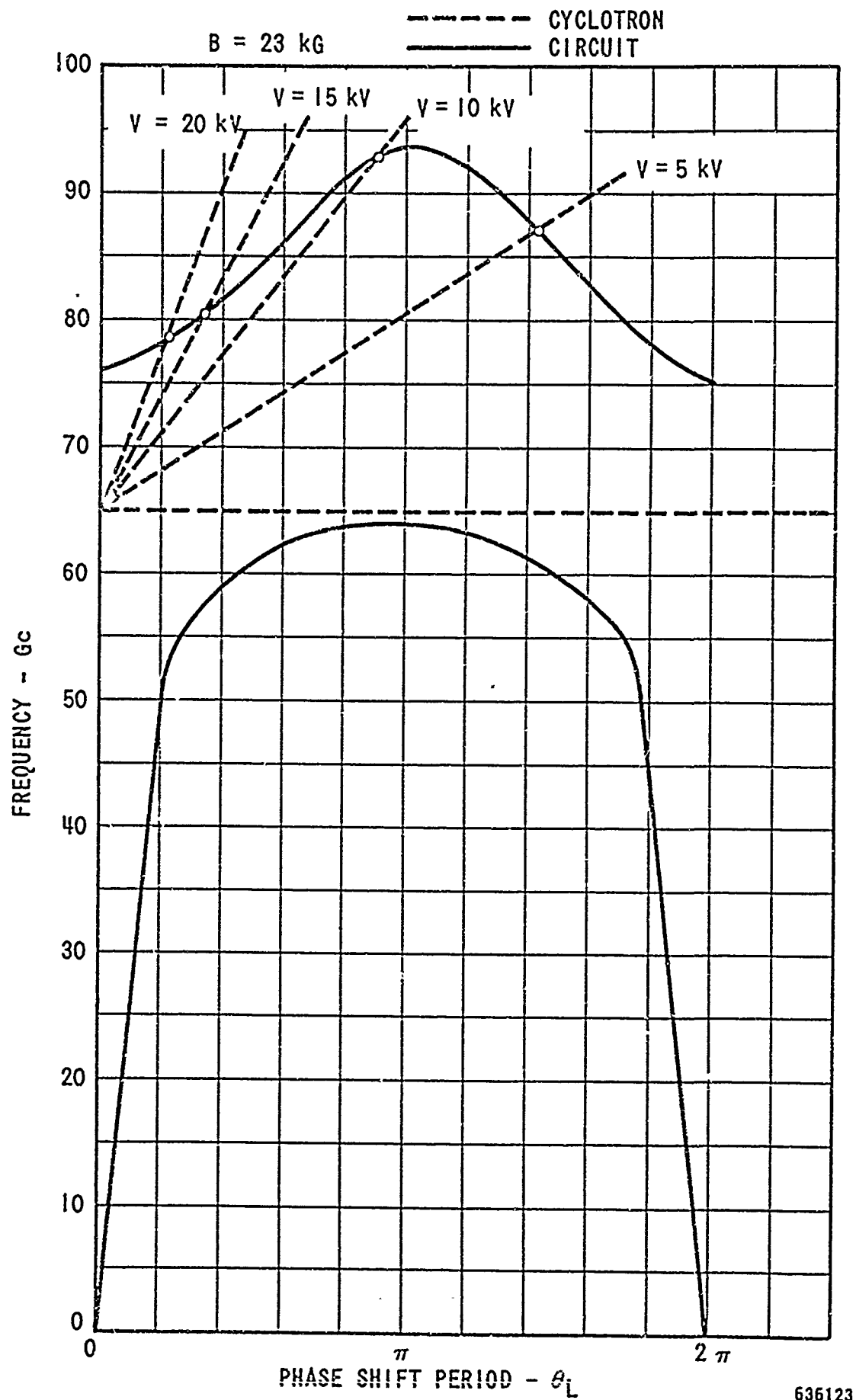Cyclotron Modes

- 42 -

lower branch can be depressed by using longer coupling slots to increase the mode separation of the two branches. As the frequency is lowered, the magnetic field need not be as high. This property simplifies the magnet requirements, but the slot radiation losses limit the length of the slot. Figure 22 shows the circuit and cyclotron phase characteristic for 23 kilogauss.

Another approach to the elimination of cyclotron interaction with the lower frequency circuit modes would be through the propagation character-istics of the network.

Perhaps a cathode design could be incorporated into the coaxial magnetron which would not support the lower order modes. As expected, when the cathode was eliminated from the cold test model, no lower order resonances were present. This fact was confirmed with the X-band cold test model. Figures 23 and 24 depict the relative amplitude of the lower order circuit modes for the anode with a solid metal cathode. The same information is plotted for the model without the cathode in Figure 25. No lower modes were detected. These data illustrate that the cathode was an essential element in the propagating structure for the lower order modes. When a special cathode was constructed with 4 metal segments, each separated by a dielectric, this network did not support the lower order modes.

A less desirable solution to the problem would be to incorporate a damper into the cathode surface.

Several cold test cathodes were made which included damper material. The most successful cathode design (#2) is shown in Figure 26. The relative amplitudes of the lower order modes, as determined in cold test, are given in Figure 27. This plot indicates that this cathode damper was effective in attenuating the lower anode circuit modes. These modes were further attenuated by the addition of the anode damper ring. The results of the addition of the damper ring are illustrated in Figure 28.

FIGURE 22 V-Band – ω–β Diagram with Fast
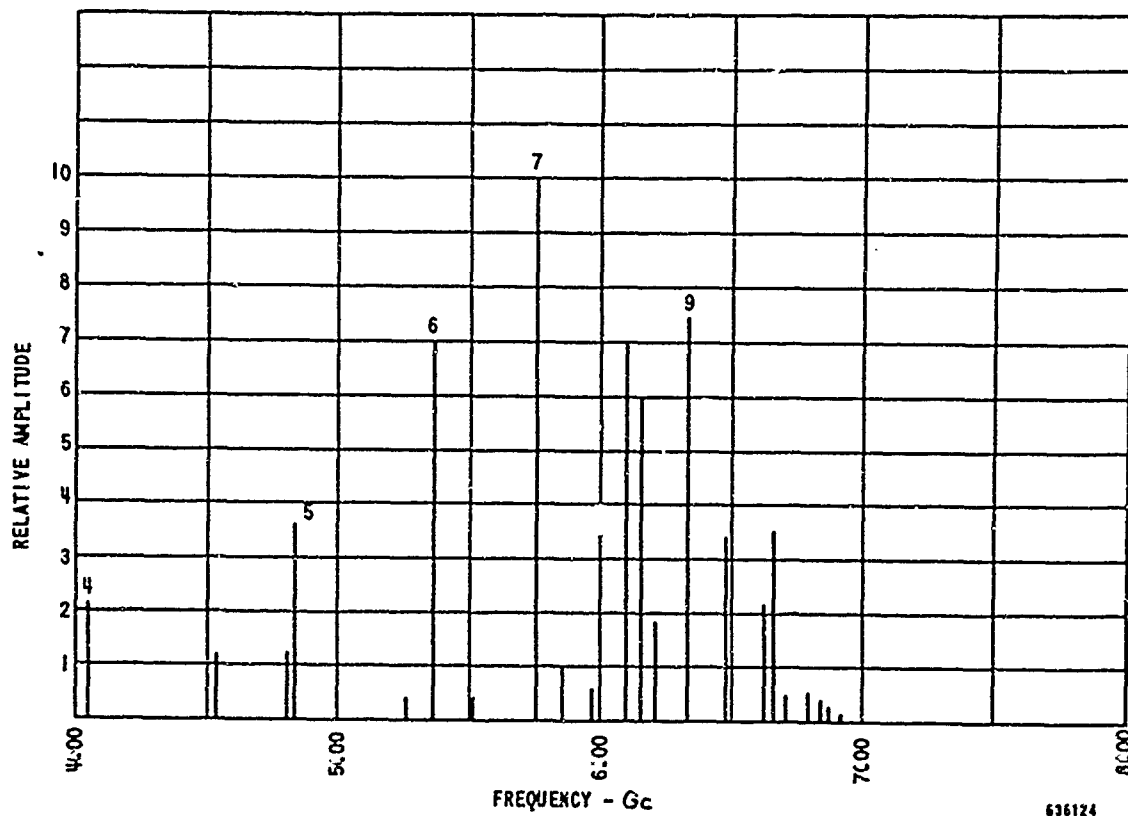Cyclotron Modes

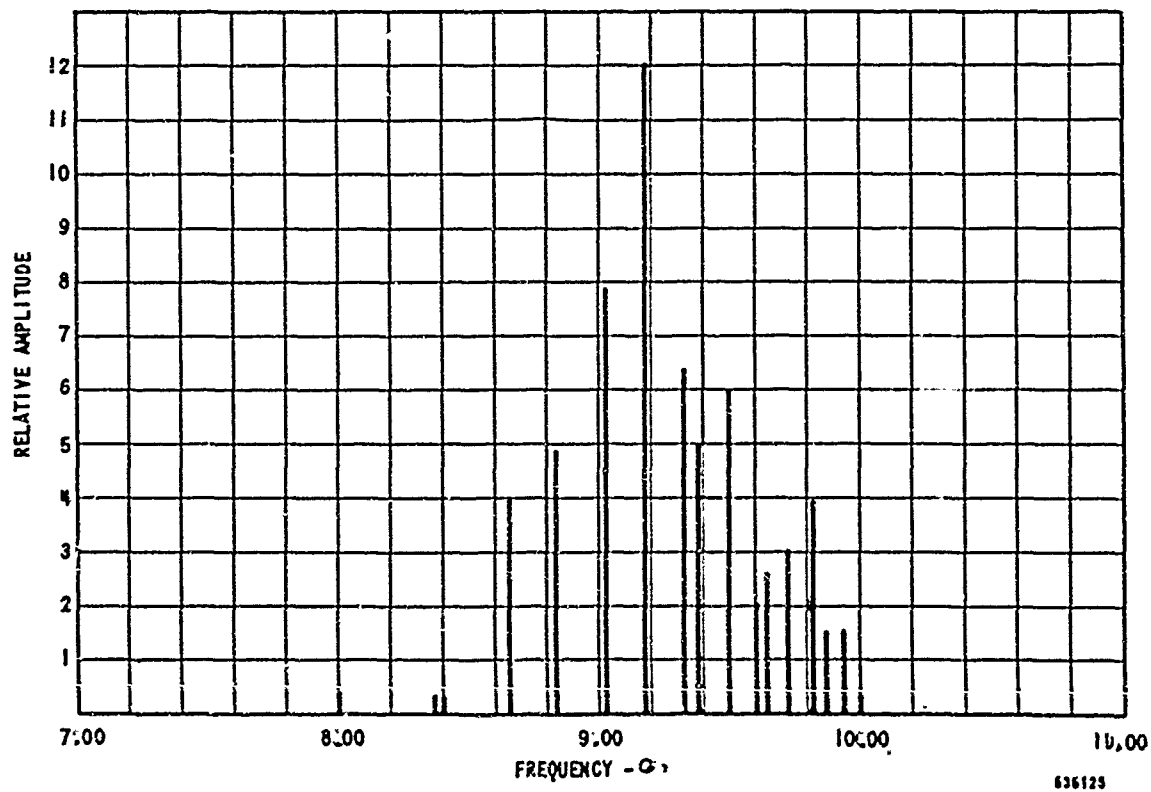Figure 23   Relative Amplitude of Lower Order Modes
With Cathode Ring

Figure 24   Relative Amplitude of Higher Order Modes
With Cathode Ring
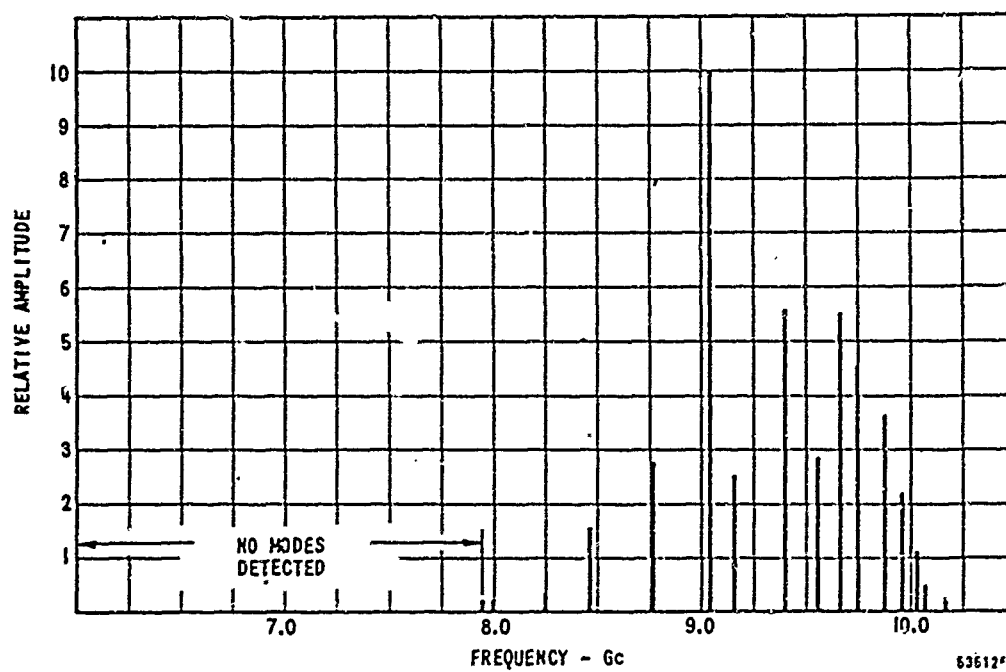
Figure 25   Relative Amplitude of Circuit Modes Without a Cathode
(Unslotted Anode)
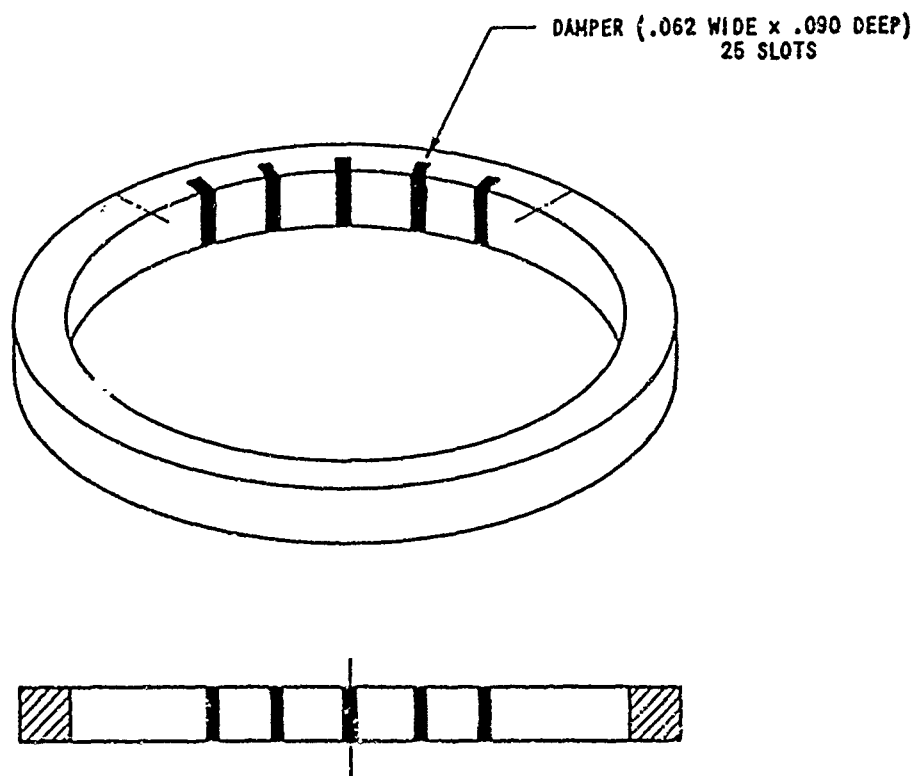
Figure 26   Special Cathode Ring #2

CATHODE RING - 25 SLOTS - .062" WIDE - .090"DEEP FILLED WITH DAMPER
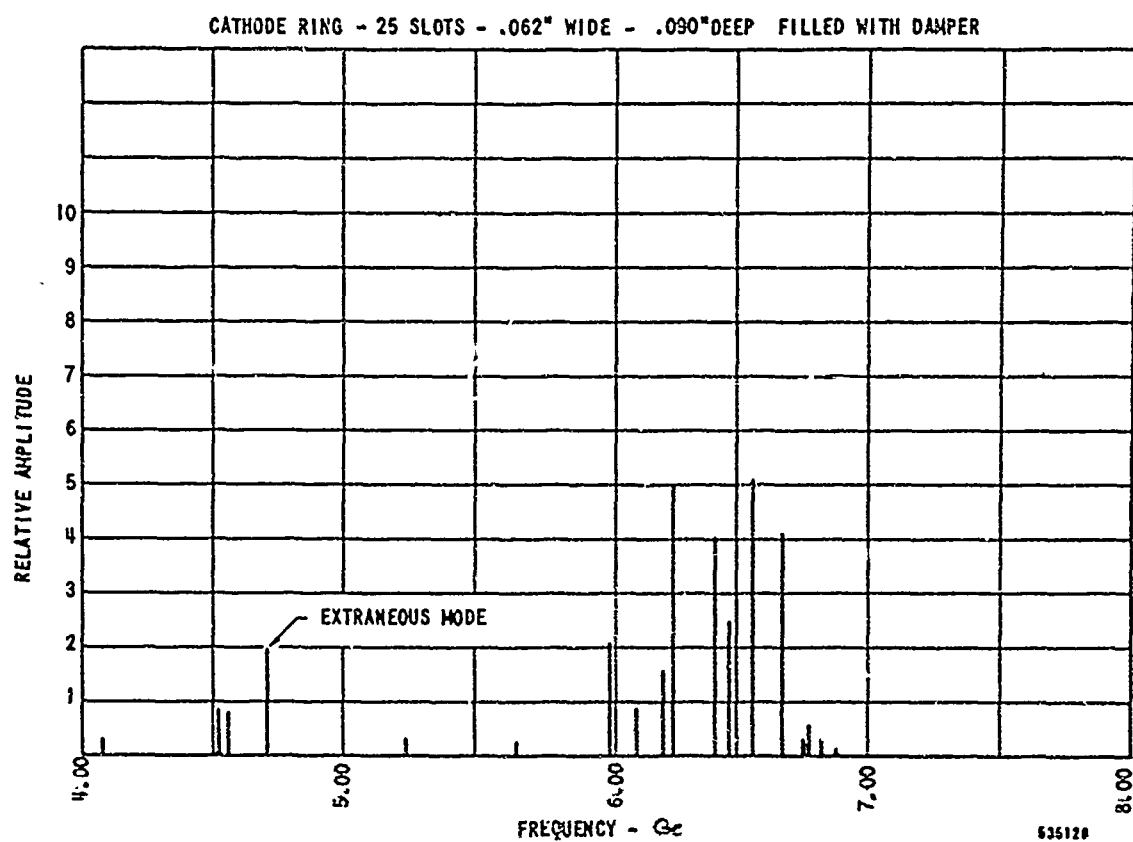
Figure 27   Suppression of Lower Order Modes
With Cathode Damper

CATHODE RINGS - 25 SLOTS- .062" WIDE - .090" DEEP   FILLED WITH DAMPER
ANODE DAMPER RING #1 - .050" FROM ANODE

Figure 28   Suppression of Lower Order Modes
With Cathode and Anode Dampers

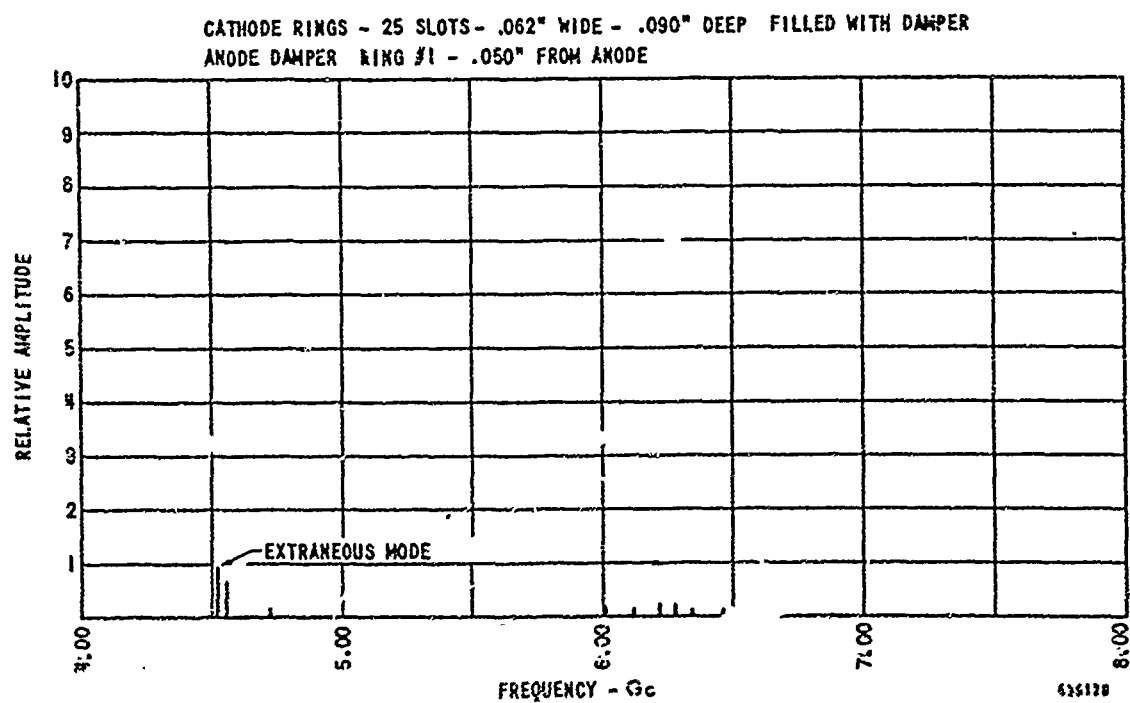This suppression of lower order circuit resonances was accomplished with the introduction of lossy materials to achieve selective loading. However, the unloaded Q of the TE_{011} cavity mode decreased as a result. In Figure 29, the unloaded Q's are plotted for solid metal and damper-cathode ring. The unloaded Q's are given for the X-band model with cathode #2 (damper) and with the anode damper at various axial positions. (See Figure 30.)

From the above information, it can be seen that there are several possible solutions to solving the cyclotron mode interference in coaxial millimeter magnetrons.

4.5 V-Band Cold Test

4.5.1 V-Band Output

During the first part of the program, a half-wavelength ceramic TE_{01} circular window assembly having a window thickness of 0.195 inch was made and cold tested. However, the bandwidth of the X-band transducer was not good enough to develop a well-matched window at this frequency. It was decided, therefore, that a separate V-band output and window design would be worked out to insure that a wide range match would be obtained at V-band.

Several V-band $\lambda/2$ ceramic windows of different thicknesses were cold tested. The cold test setup was not ideal, however, since no circular TE_{01} matched load was available. As a result, a rectangular waveguide load was used, and the setup required 2 rectangular-to circular transducers. These transducers were not well matched at 93.75 Gc.
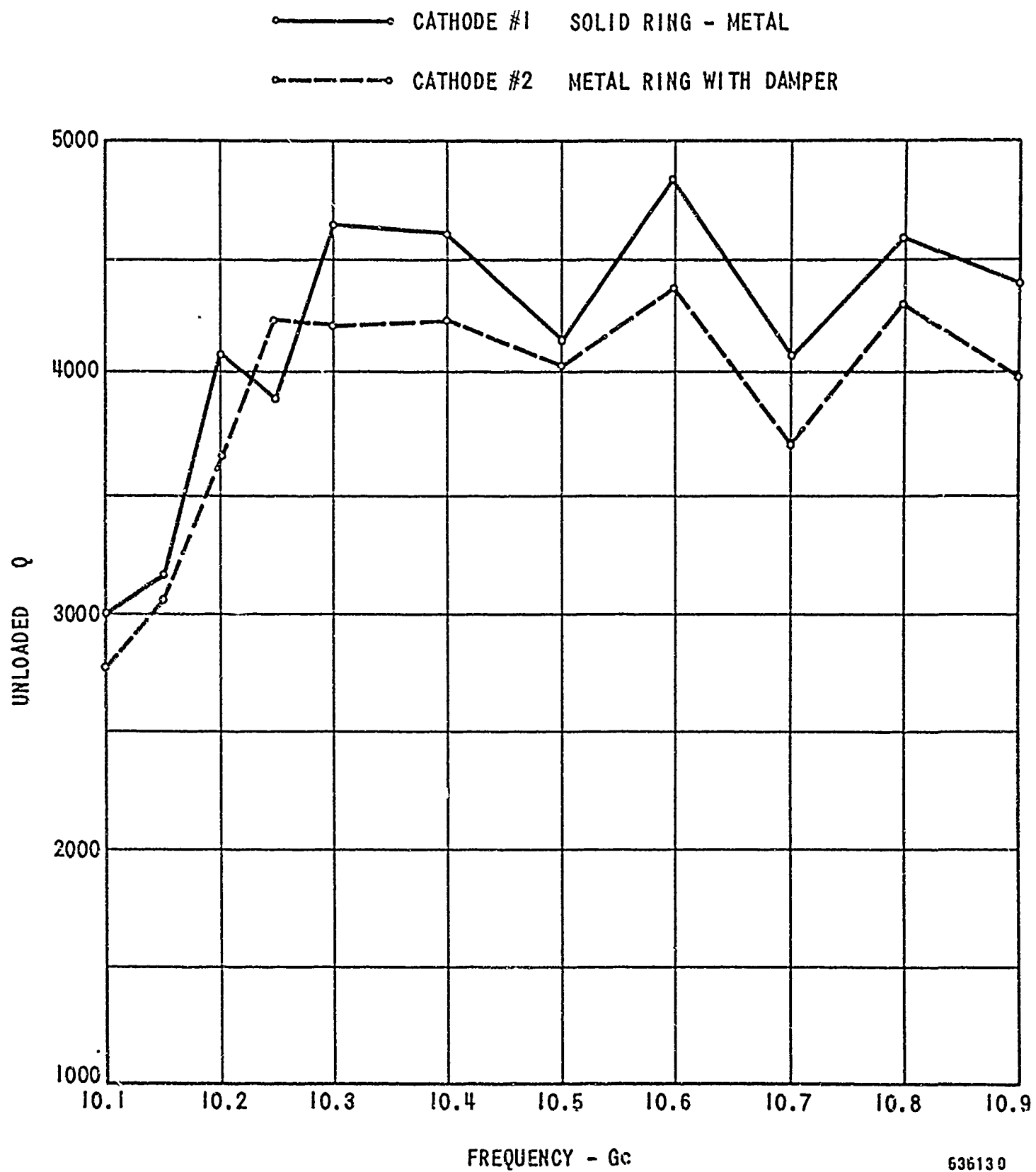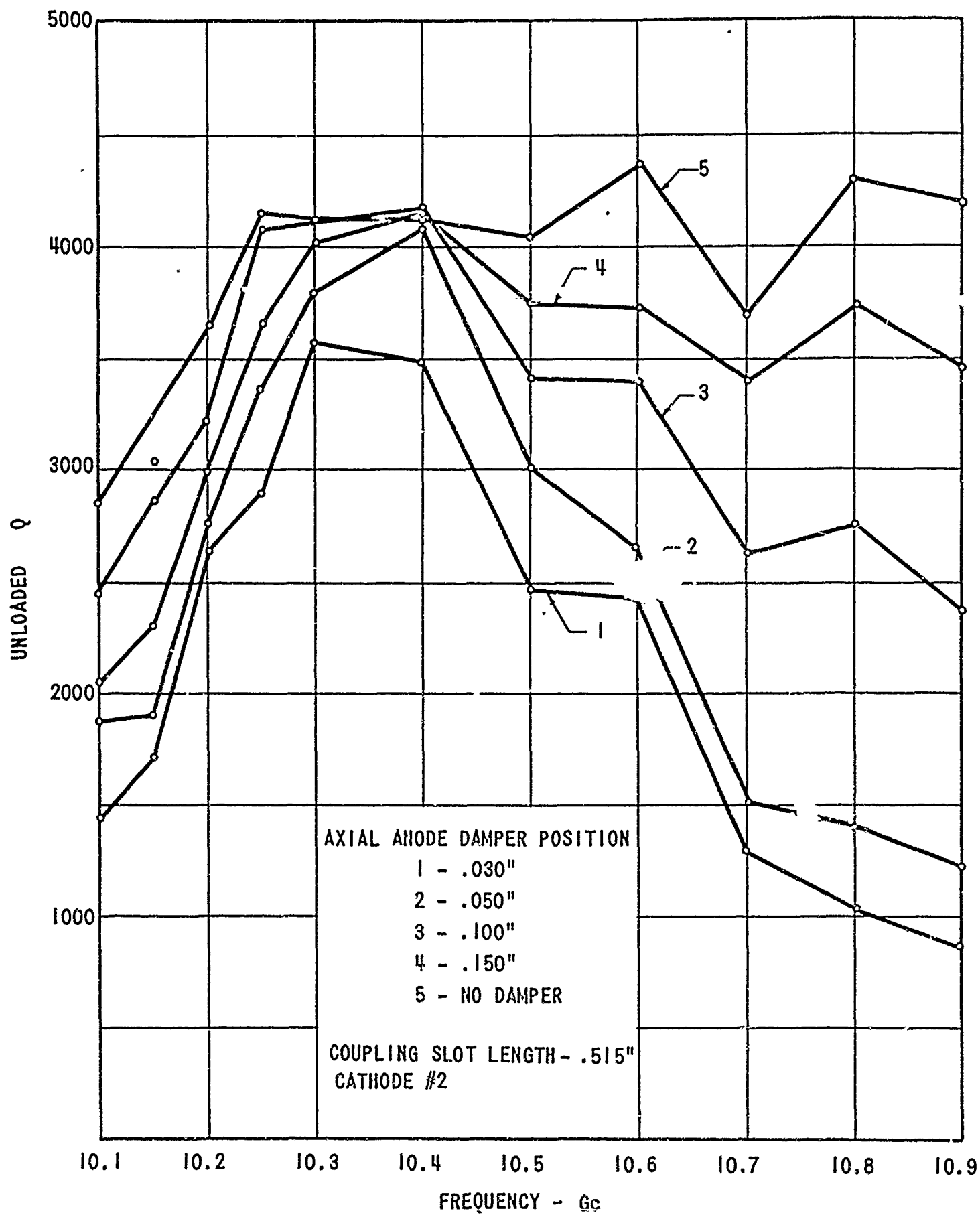
FIGURE 29   TE$_{611}$ Mode Unloaded Q vs Frequency

636130

FIGURE 30 TE$_{011}$ Mode Unloaded Q for Various Axial Positions of Anode Damper

636131

Two 3° circular tapers were cold tested back to back. The VSWR of the tapers was satisfactory. A taper is needed in the tube to provide a transition from the tube output to the standard V-band circular waveguide Figure 31 gives the cold test results for two $\lambda/2$ ceramic windows 0.0195 inch and 0.022 inch thick. From these data, it can be concluded that a matched window has been developed.

4.5.2 Anode-Cavity Cold Test

The V-band anode-cavity was also cold tested and a cold test model of the cathode and tuner was made.

An unloaded Q of 1100 was measured with this model. A tuning curve was also taken. This unloaded Q was considered adequate.

4.6   Electro-Mechanical Aspects

4.6.1 V-Band Output

Several V-band windows were assembled and brazed in specially constructed jigs. After brazing, the windows met the dimensional specifications.

4.6.2 V-Band Anode

A V-band anode was fabricated by Triangle Tool and Die Company of Lynn, Mass., by E. D. M. (Electrical Discharge Machining) method. The anode met all dimensional specifications. These dimensions were checked on an optical micrometer. Figure 32 shows the V-band anode, micrometer tuner and output assemblies. Figure 33 depicts the details of the V-band anode.

636132
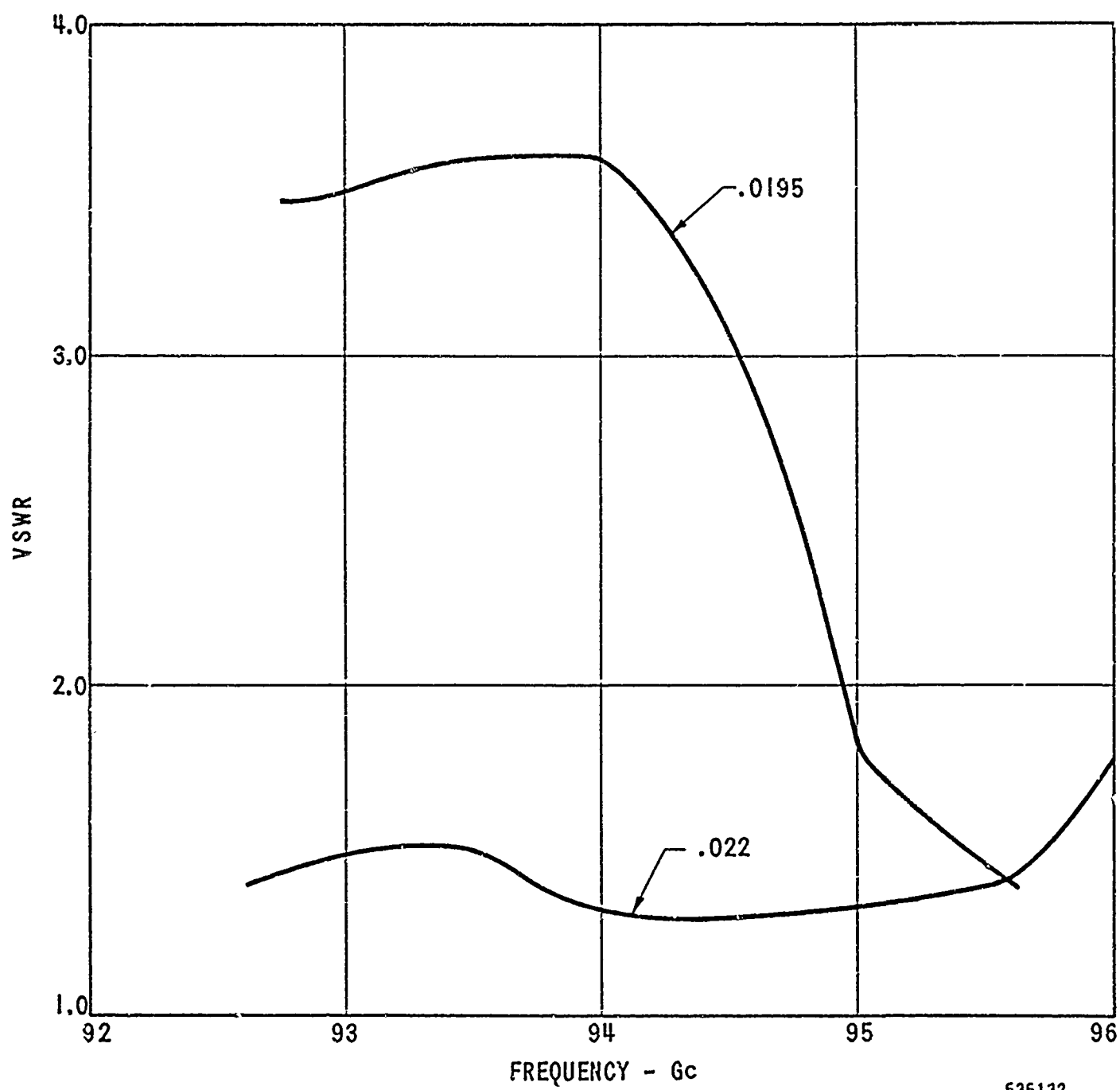
FIGURE 31 $\lambda/2$ TE_{01} Ceramic Window - VSWR

Cathode and Pole Retainer Block

Tuner Head

Tuner Plate and Post

Anode-Cavity

Pole and Output Assembly
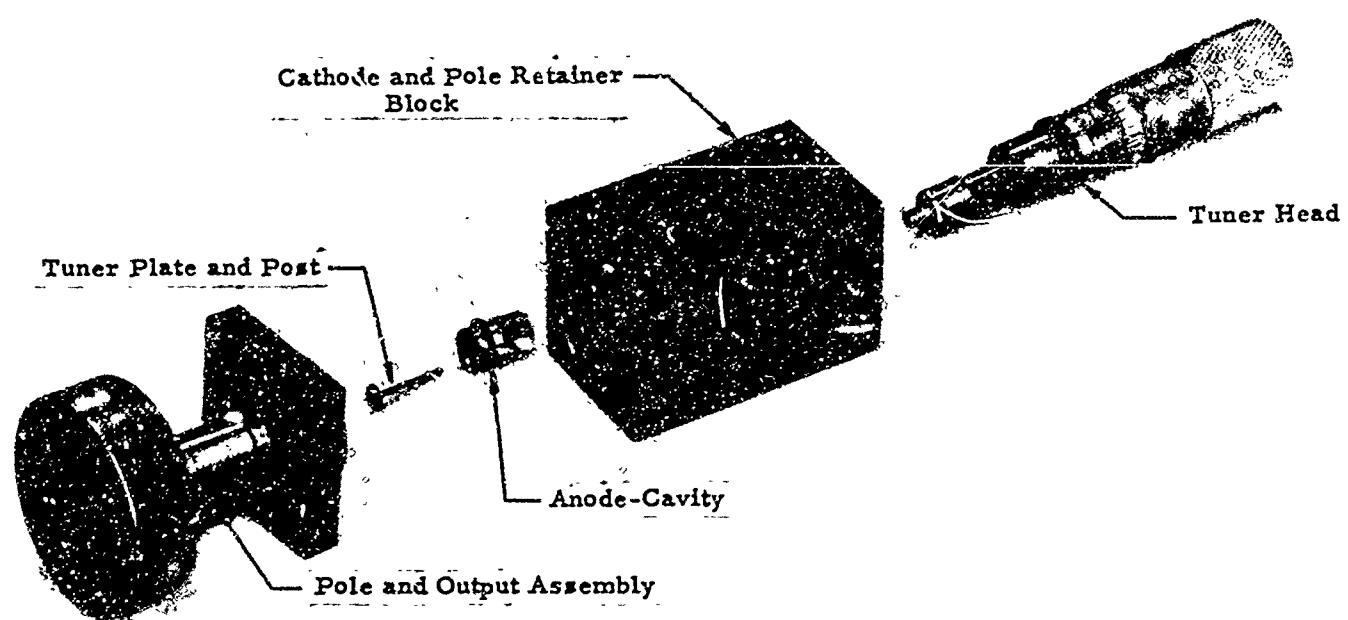
65-25277

Figure 32   V-Band Anode, Micrometer Tuner
and Output Assemblies

65-25278

Figure 33   V-Band Anode

4.6.3 Magnetics

The pole gap of the V-band tube is 0.150 inch and the area of the pole is 0.08 in^2. The design requires a magnetic field of about 22,000 gauss across this gap. It was recognized that permendur pole pieces would be needed to carry the required flux. Experiments were made with various shapes and types of permendur before a satisfactory design was obtained. Vanadium permendur was first used but produced only 15,200 gauss before saturation occurred. Later heat treatment of this material gave some improvement to 17,500 gauss at saturation. Further changes in pole geometry with vanadium permendur did not significantly alter the magnetic field. An improved material with greater flux carrying capability was then obtained, known as 2V supermendur. Resulting measurements of the flux across the interaction space made on an electromagnet are shown in Figure 34. Pole gaps of 0.120 inch and 0.180 inch were used. With the particular electro-magnet employed, a current of 2.0 amperes will produce the required 22,000 gauss across an 0.150 inch gap. It is estimated that the final design tube can be packaged in magnets weighing 40 pounds to provide the desired magnetic field.

4.6.4 Damper

High alumin carburized ceramic dampers were used on the X-band anode model to attenuate the vane and coupling slot modes. The V-band cold test unit was to have dampers of the same material fabricated in a manner to hold the close spacing required between the copper anode and the inside surface of the damper. This technique was not successful, however, and an alternate method to hold the damper for hot test V-band tubes will need to be used. The method called for segments of ceramic to be brazed into a copper retainer, with the resulting assembly ground to fit the anode cavity outside diameter. Following this operation, the retainer with ceramics was to be slipped onto the anode and welded in place. The ceramic was segmented so that differential expansion of copper and ceramic would not prevent the ceramic from following the expansion of
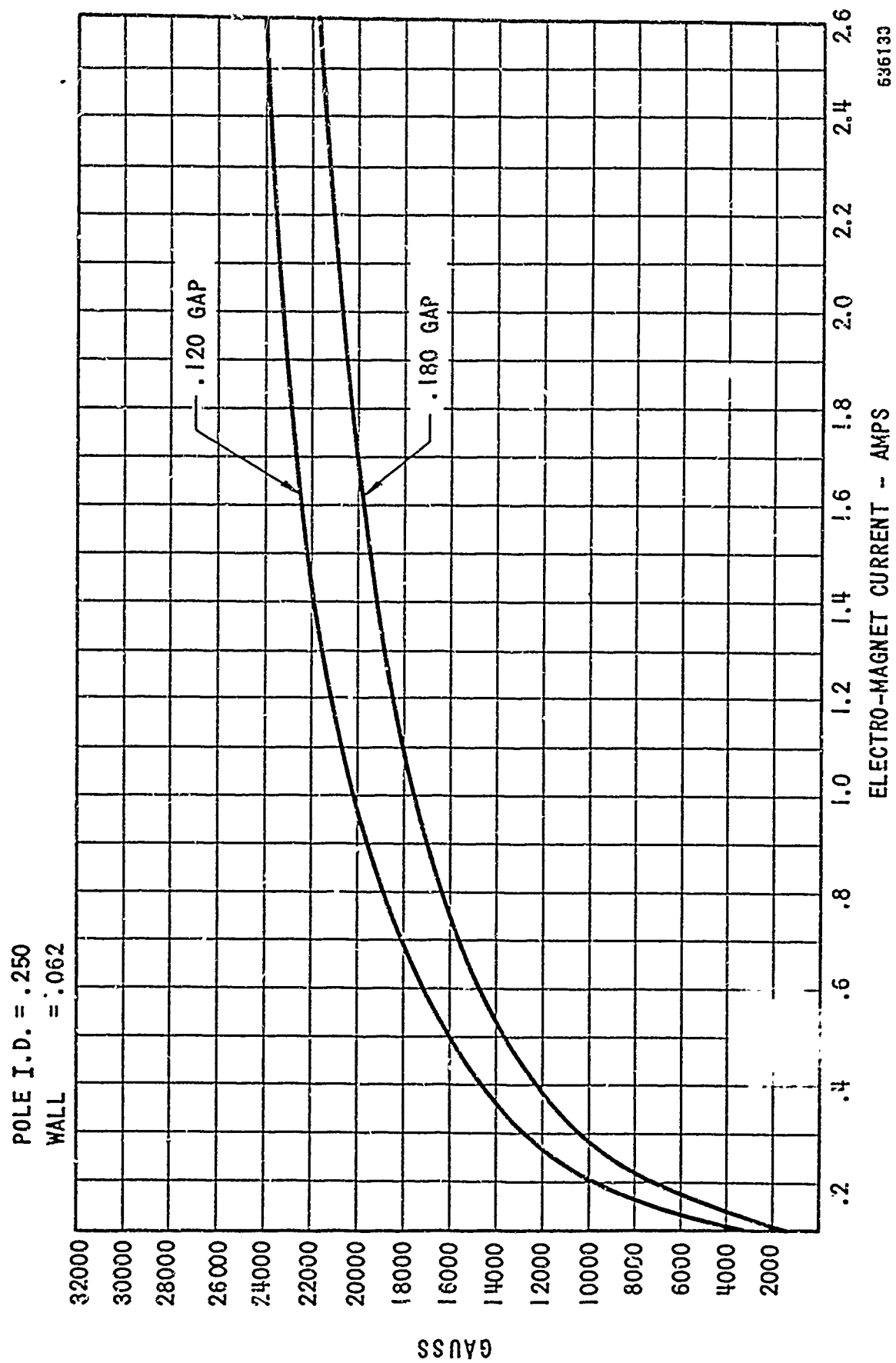
POLE I.D. = .250
WALL   = .062

.120 GAP

.180 GAP

ELECTRO-MAGNET CURRENT ~ AMPS

GAUSS

FIGURE 34   QKH1.334   2V Supermendur Poles

636133

- 56 -

the anode and copper retainer. It was thus felt that the damper could remain in intimate contact with the anode over a wide temperature range and without damage or distortion of the anode.

Difficulty was encountered in grinding the ceramic to the thin wall dimensions required (0.005 inch) and in maintaining a metalized surface on the ceramic during the slotting operation. The later problem could have been overcome by metalizing and carburizing individual segments after slotting. However, the first limitation, cracking of the ceramic when grinding to thin walls, prevented successful fabrication of the damper assembly. Several attempts were made to grind the ceramic, which were packed in a plastic casing to dampen interaction but cracking occurred in all cases as the wall thickness was reduced below 0.010 inch.

It is planned that the damper design be modified during subsequent development work to remove the cracking of the ceramic. The technique which will be followed involves the use of a sprayed alumina coating put onto the inside diameter of a slotted tungsten sleeve. The resulting unit would then be carburized and slipped over the anode where it will be held in close contact with the slots.

4.6.5 Cathode Heater Design

The heater cathode assembly which was evaluated for use with the tube is shown in Figure 35. The heater is formed in the shape of a rosette and coated with alumina. It is placed flat in the cathode assembly and insulated on all four sides with ceramic liners. A tungsten aluminate cathode is brazed to the inner diameter of the heater box, and heat reflecting end shields are attached at the outer diameter. The entire assembly is self jigging and held together by electron beam welding.
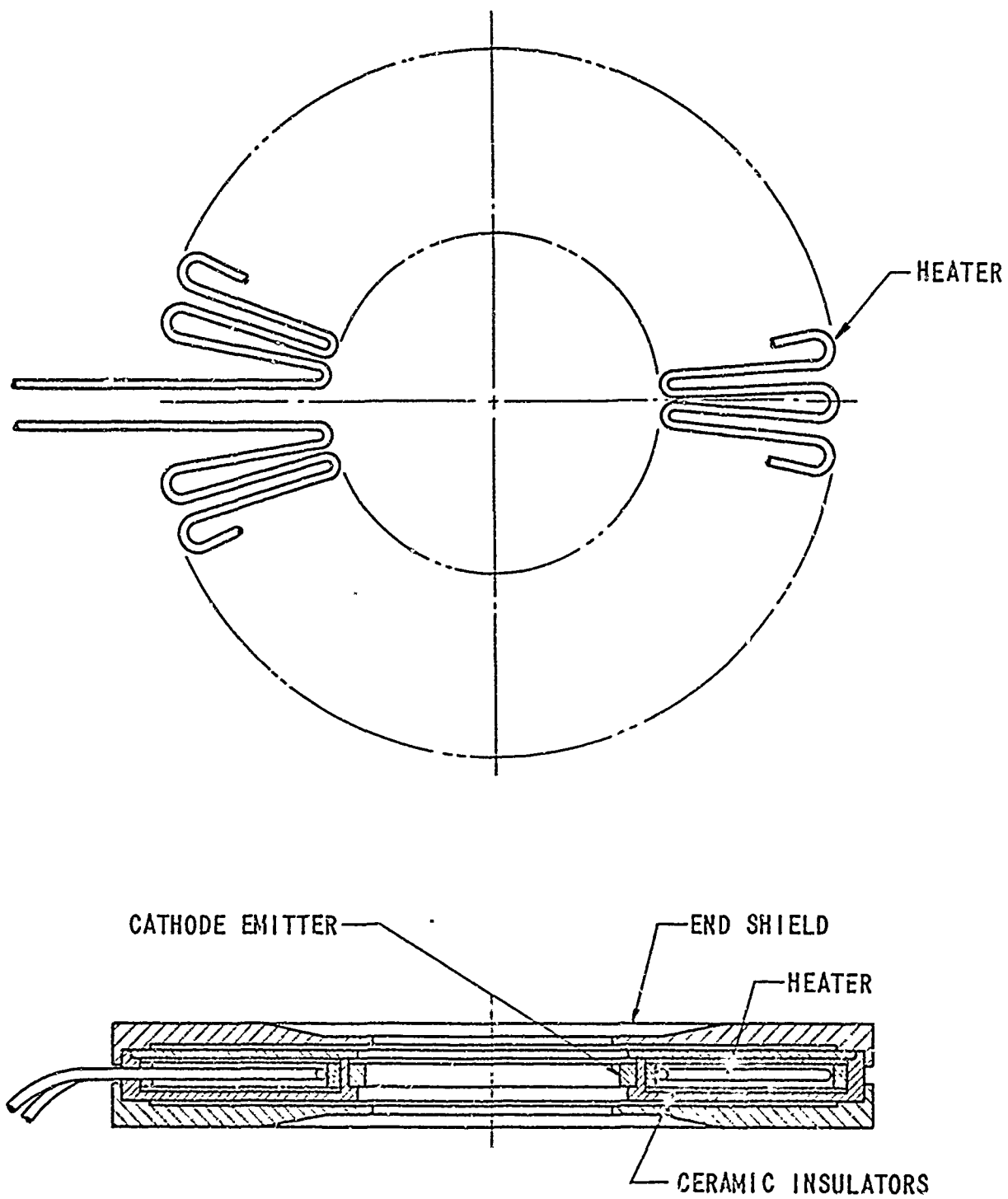
FIGURE 35   Heater Cathode Assembly

A model of the heater cathode was assembled and tested in a
vacuum bottle. Power input of 30 watts at 11 volts was needed to
attain an operating temperature of 1050°C. The unit was cycle life tested
to 1040 hours, at which time it was removed. No short circuits
occurred during 500 cycles of operation and the design is considered
satisfactory. A magnetic field could not be applied during the testing,
and the effects of this force on the heater have therefore not been
evaluated. Although there will be a high field in the operating tube,
the manner in which the heater is coated and retained in the cathode
should prevent short circuits from developing.

5.   SUMMARY AND CONCLUSIONS

A general analysis of an inverted coaxial magnetron was carried out in this program. It was directed towards solving problems that would arise in a millimeter tube. An X-band cold test model (9-scale version of the V-band) was made. The cold test work on this model was extensive. Nearly all the information obtained at X-band can be scaled to V-band. Slot and circuit modes can be explained by assuming the coaxial magnetron to be a modified rising sun type. The cold test results confirmed this assumption.

Means of attenuating the undesired modes were developed. For adequate attenuation, it was found that the anode damper must lie in close proximity to the anode cylinder. Therefore, a V-band damper must be precisely made. The anode-to-damper fit also would need to be maintained under all operational conditions.

The factors that influence the unloaded Q of the cavity-anode were examined, These factors included slot length, dampers, iris coupling and presence of circuit modes. It was found that the unloaded Q could be raised especially through selective loading.

Also the output coupling problem was investigated. This information will be useful for V-band design.

The problem of the beam cyclotron wave interaction with the circuit wave was also carefully examined. This interference is a serious design problem in millimeter crossed-field microwave oscillators.

Several solutions to the cyclotron interference were examined. Operation at high magnetic field prevents lower frequency cyclotron interaction. If the magnetic field is such that the cyclotron frequency is greater than highest frequencies of the lower circuit modes, cyclotron interaction will not take place with these circuit modes.

By the inclusion of dampers in the cathode, the lower circuit modes were strongly suppressed. Thus, this additional dampening would tend to eliminate cyclotron interaction. Also, modification in the cathode structural design such that the lower order circuit modes are not excited would be another possible solution. Cyclotron mode interference with higher frequency circuit modes will be controlled by anode dampers.

A V-band anode-cavity assembly was made by E. D. M. method. It met all dimensional specifications. The measured unloaded Q of 1100 is adequate. A V-band $\lambda/2$ ceramic window was developed. The match on this window was satisfactory with the use of supermendur. A magnetic flux for the V-band model of 22,000 gauss was obtained. Although a V-band damper design was worked out, technical problems arose in the actual fabrication of the damper. Means of resolving these problems are apparent. A heater-cathode assembly was made and cycle life tested for 1040 hours at 30 watts (input power = 1050°C). Thus, the design of the cathode-heater was satisfactory.

6. RECOMMENDATIONS

This program will serve as ground work for a second phase of the V-band program which includes the building and testing of V-band tubes. From the X-band cold test work, all of the various mode interference problems can be solved at V-band. Several approaches to the solution of the cyclotron interaction problem are available.

Several of the electro-mechanical aspects of this V-band anode have been developed. A V-band anode cavity was successfully fabricated by E. D. M. method.

In phase II, it is proposed that a demountable system be employed in evaluating the tubes to allow variations in the design to be carried out rapidly on a single tube.

7.   IDENTIFICATION OF ENGINEERS

This program was carried out under the general supervision of Mr. Lawrence Clampitt, Manager of Engineering, Microwave Tube Operation, in the Microwave and Power Tube Division, and Mr. James Schussele, Manager of the Crossed-Field Oscillator Group. The program was assigned to the Magnetron Laboratory headed by Mr. Edward T. Downing. Engineering effort was accomplished by Mr. Robert Plumridge, Senior Engineer and Mr. John R. Butler, Engineering Section Head. Mr. William Bowers was responsible for the initial design of the tube and for an analysis of engineering problems peculiar to the inside-out magnetron.